SUPPLEMENTARY MATERIALS FILE

Loss of ADAMTS9 disrupts ciliogenesis and collagen homeostasis resulting in Nephronophthisis-like polycystic kidneys

Sydney Fischer[1], Karyn L. Robert[1], Manu Ahmed[1], Griffin I. Kane[2,3], Matthew A. Kavanaugh[4], Wei Wang[4], Pamela V. Tran[4], Prabhani U. Atukorale[2,3] and Sumeda Nandadasa[1*]

SUPPLEMENTAL METHODS

Mice

The mice were housed under a 12-h light and 12-h dark cycle and had unrestricted access to food and water. The *Tmem67*$^{+/-}$ mice (C57BL/6NJ-*Tmem67em1*$^{(IMPC)J/Mmjax}$) were purchased from the Jackson Laboratory (JAX, 051248). *Tmem67*$^{\Delta CLE/+}$ founder mice were generated in the C57BL/6J background by Cyagen (Santa Clara, CA) as previously described (1). The *Ift88*^{Fl} mice were purchased from Jackson Laboratory (JAX: 022409). *Adamts9*$^{Fl/+}$ and *Adamts9*$^{Del/+}$ mice (2, 3) were obtained from Dr. Suneel Apte and were maintained in the C57BL/6J background. *Six2*-Cre eGFP mice were obtained from the UT Southwestern, George. M O'Brien Kidney Research Core Center, and were maintained in a mixed background of C57BL/6J, Swiss Webster and FVB (4). *Ksp*-Cre mice were purchased from Jackson Laboratory (JAX: 012237). *Vcan*$^{Fl/+}$ mice (*Vcan*$^{tm1.1Cwf}$) (5), were provided by Dr. Charles Frevert and Thomas Wight. *Vcan*$^{Hdf/+}$ (null-allele) and *Vcan*$^{AA/+}$ mice (6, 7) were provided by Dr. Suneel Apte and were maintained in the C57BL/6J background. *Pkd1*^{Fl}, *Pkd2*^{Fl}, *HoxB7-Cre* and *ROSA26-Cre*^{ERT} mice were purchased from Jackson Laboratory (JAX, 010671, 017292, 004692, 004847) and maintained on a C57BL/6J background. *Pkd1* cKO mice were analyzed at P14. To generate *Pkd2* cKO; *ROSA26-CreERT* mice, nursing mothers were injected intraperitoneally with tamoxifen (8mg/40g; Sigma-Aldrich, T5648) at P0 to induce gene deletion. Offspring were analyzed at P21. A list of genotyping primers used to genotype each mouse line is provided in Supplemental Table 1.

Cell Culture

Primary kidney cell cultures were established from mouse kidneys at postnatal day 14 or 21. In brief, kidneys were finely minced and digested in 1.5% Collagenase IV for 1 hour (hr) at 37°C. Cells were cultured in media containing DMEM/F12 (Gibco;11330-032;), 2% FBS, 200 U/mL penicillin/streptomycin (Gibco; 15140-122), glutamine, 5 mg/L human transferrin, 5 mg/L

recombinant human insulin, 7.5 nM sodium selenite, and 2nM 3,3,5'-Triiodo-Thyronine 2 nM at 37°C, 5% CO2 as previously described (8). Wild type HTERT-RPE-1 (ATCC, CRL-4000) and *ADAMTS9* KO RPE-1 cells (9), were maintained in DMEM/F12 (Gibco;11330-032;) with 10% FBS and 200 U/mL penicillin/streptomycin (Gibco; 15140-122) and maintained at 37°C with 5% CO_2.

Plasmid DNA constructs and transfections

The ADAMTS9 S636F, R647Q, R1203W, C1024*, P1665S and S1826N patient variants were generated using the Q5 Site-Directed Mutagenesis Kit (NEB; E0554S) using the full-length ADAMTS9 plasmid construct in the pCDNA3.1Myc/His backbone described previously (9) utilizing the primers listed in Supplemental Table 2. T65R and Q1525Hf/s variants were previously generated in the pENTER backbone (10). All constructs were verified through Sanger sequencing. For plasmid DNA transfections, RPE-1 cells were transfected with 300 ng of plasmid DNA per well in 8-chamber slides (Corning; 354118) grown at 60-80% confluency, using PEI MAX transfection reagent (Polysciences; 24765). Transfected cells were washed by PBS and serum starved for 24 hrs by culturing in serum-free DMEM/F12 culture medium, for ciliogenesis and TZ analysis.

Western blot analysis

Confluent primary kidney cell cultures or RPE-1 cultures in 6-well plates were serum starved for 48 hours in 1 ml of serum-free DMEM/F12 culture medium and lysed using 300 μL Transmembrane lysis buffer (FIVEphoton biochemicals; TmPER-50) as previously described (1). 6x Laemmli sample buffer was used for boiling cell lysates or conditioned medium for 10 min at 100 °C. Samples were loaded on to 7.5% acrylamide gels and electrophoresed for 60-90 minutes at 110V. Protein bands were transferred to Immobilon-FL transfer membranes (EMD Millipore, IPFL00010) for 3 hrs at 333 mA at 4 °C, and subsequently blocked with 5% nonfat dry milk dissolved in PBSTw (PBS+ 0.1% Tween-20) for 1 hour. Primary antibodies were diluted in

5% nonfat milk and incubated overnight at 4 °C with agitation. Li-Cor fluorescent secondary antibodies were diluted in PBSTw and incubated for 2 hrs at room temperature (RT) following 3x PBSTw washes. Western blot membranes were imaged using the LI-COR Odyssey M scanner. Western blot band intensities were quantified using NIH Image J (FIJI). A list of all antibodies and dilutions used in western blotting are provided in the key resource table (Supplemental Table 4**)**.

Immunostaining and fluorescent microscopy

Dissected mouse kidneys were bisected and fixed overnight at 4°C in 4% PFA. For cryo sectioning, immediately following 3x PBSTw washes, fixed samples were placed in 15% sucrose overnight followed by 30% sucrose at 4°C overnight. Samples were imbedded in OCT (Tissue-Tek; 4583). Cryo-embedded kidneys were sectioned via a Leica CM 1950 cryostat collecting 7 μm frozen sections. For paraffin sectioning, fixed kidneys were washed 3x in PBSTw following fixation and paraffin embedded using standard procedures. A Leica RM2155 motorized microtome was used for collecting 7 μm paraffin sections. Deparaffinized paraffin sections and rehydrated cryo sections in PBS were blocked with 5% NGS in PBSTx (PBS+ 0.1% Triton X-100) for 2 hrs. Kidney sections were incubated overnight at 4°C with primary antibodies diluted in blocking buffer. Sections were washed 3x with PBSTx and incubated in secondary antibodies diluted in PBS for 2 hrs in the dark at RT. Following 3x PBSTx washes, the slides were mounted in Prolong gold antifade mounting media containing DAPI (Invitrogen; P36931). For immunostaining primary kidney culture and RPE-1 cells, serum starved cells grown in 8-chamber slides (Corning; 354118) were fixed with ice cold methanol for 5 minutes at -20°C for TZ analysis or 4% PFA for 30 minutes at RT for cilium staining. Cells were washed 3x with PBSTw and blocked for 2 hrs in 5% NGS made in PBSTw. Primary antibodies were diluted in blocking buffer and incubated overnight at 4°C with agitation. After 3x PBSTw washes, the cells were incubated with secondary antibodies diluted in PBSTw for 2 hrs at RT. After 3x

PBSTw washes, the slides were mounted with Prolong gold antifade mounting medium containing DAPI (Invitrogen, P36931), and curated overnight at RT. Confocal images were obtained using a Leica SP8 laser scanning confocal microscope with a 63x 1.47 N.A. oil-immersion objective, a 40x N.A. 1.30 oil objective, or a 20x N.A. 0.75 dry objective. Whole kidney fluorescent images were obtained utilizing a TissueGnostics TIssueFAXS microscope. A list of all antibodies and dilutions used in immunostaining are provided in the key resource table (Supplemental Table 4**)**.

Cystic kidney histopathology assays

Dissected mouse kidneys were bisected using a sharp razor blade and fixed overnight at 4°C in 4% PFA and then washed 3x with PBSTw. Fixed kidney samples were then dehydrated over two consecutive nights, in 50% ethanol and then 70% ethanol at 4°C. Kidney samples were embedded in paraffin using a standard tissue processing procedure. Kidney sections were cut at 7 μm using a Leica RM215 motorized microtome. For hematoxylin and eosin staining, sections were deparaffined and stained with eosin Y 1% (VWR; 10143-130) and hematoxylin (VWR; 10143-142) and mounted in Cytoseal XYL medium (Adwin Scientific, NC9527349). For Masson's Trichrome staining, kidney sections were deparaffined and refixed in Bouin's fixative (Electron Microscopy Sciences (EMS); 26367-01), stained with Weigert's iron hematoxylin A & B solutions (EMS; 26367-02 and -03), Biebrich scarlet solution (EMS; 26367-04), and aniline blue solution (EMS; 26367-06) followed by a 5 minute 1% acetic acid (EMS; 26367-07) fixation. For Periodic Acid Schiff (PAS) staining, slides were deparaffined followed by staining with 1% periodic acid (A223-25, Fisher), Schiff's reagent (26853-01, Electron Microscopy), and Mayer's hematoxylin (Volu-Sol, VMH032). All samples were mounted in Cytoseal XYL medium and imaged using a TissueGnostics TIssueFAXS slide scanner or a Zeiss Axioplan microscope equipped with a Leica DM6200 camera.

Quantitative real time PCR (qRT-PCR)

mRNA was harvested from whole mouse kidneys snap frozen in 500 μL Trizol reagent and crushed into a fine powder using a frozen pestle and motor. The thawed lysates was sonicated for 30 seconds followed by chloroform extraction and isopropanol precipitation. RNA pellets were washed with 100% and 70% ethanol and resuspended in nuclease-free water. 2 μg of mRNA per sample was used in cDNA synthesis using the High Capacity cDNA Reverse Transcription Kit (ThermoFisher; 4368814). A BioRad CFX connect real time PCR machine was used in combination with Bullseye EvaGreen qPCR master mix (Midsci; BEQPCR-R) for determining ΔCT values. Each sample was run in duplicate with at least 4 experimental replicates per group. All gene expression data was normalized to *18s*. A list of qRT-PCR primers used in this study are provided in Supplemental Table 3**.**

Transmission and Scanning Electron Microscopy

All EM samples in this study were processed and analyzed at the University of Massachusetts Chan Medical School Electron Microscopy core facility according to standard procedures. In brief, mouse kidneys were fixed in 2.5% glutaraldehyde with 1.6% paraformaldehyde in 0.1 M sodium cacodylate buffer (pH 7.2), overnight at 4 °C. The samples were then washed 2x in fresh fixation buffer at RT and post-fixed with 1% osmium tetroxide for 1 hr at RT. Samples were then washed 2x with dH_2O for 5 min and dehydrated using a graded ethanol series (of 20% increments) and finally in two changes of 100% ethanol. Fully dehydrated samples were infiltrated with 100% propylene oxide and then with propylene oxide followed by a SPI-Pon 812 50%–50% mixture overnight. Samples were polymerized at 68 °C in plastic capsules immediately following 3x fresh 100% SPI-Pon 812 resin washes. Polymerized samples were oriented, and 70 nm ultra-thin sections were collected using a Leica EM UC7 ultramicrotome equipped with a Diatome ultra 45 diamond knife for TEM analysis. Sections were placed on copper support grids and contrasted with lead citrate and uranyl acetate. TEM analysis was conducted utilizing a FEI Tecnai 12 BT with 120 kV accelerating voltage, and images were obtained by a Gatan TEM CCD camera. For freeze-fracture SEM analysis of wild type and

cystic kidney cilia, fixed kidneys were dehydrated through a graded series of ethanol and either directly critical point dried or immersed in liquid nitrogen and placed on a liquid nitrogen-cooled block, and fractured using a pre-cooled hammer and razor blade. Fractured kidney pieces were collected and thawed in 100% ethanol and critical point dried. Kidney samples were mounted on aluminum SEM stubs with fracture surfaces pointing up and metal-coated (Au/Pb, 60/40) prior to imaging using a FEI Quanta 200 MKII FeSEM.

Flow Cytometry

Immediately following euthanasia, freshly harvested kidneys were chopped with a razor blade and placed into collagenase-containing DMEM with 10% FBS for 1 hr at 37C. The samples were then mashed through 40 micron mesh filters (Fisher Scientific; 22363547) and passed through a 27G syringe prior to centrifugation at 1,500g for 5 min. Samples were resuspended in 1 mL ACK lysis buffer (Thermo Fisher; A1049201) for 10 min followed by an additional wash with 1 mL ACK lysis buffer. The concentration of cells were determined using a Countess 3 cell counter (Invitrogen) and resuspended in FACS buffer, and plated at 1 million cells per well in 96-well clear round-bottom plates for immunostaining. Fc block (BD Biosciences; 553142) diluted 1:50 in FACS buffer was added prior to staining at 4C for 30 min using 1 μg per well of each of the following fluorescently tagged primary antibodies in 100 μl FACS buffer. All primary antibodies and their dilutions used in flow cytometry assays are provided in the key resource table (Supplemental Table 4). Cells were stained with DAPI (1:1000 in FACS buffer), then washed 3x with PBS and resuspended in PBS before analysis on a ZE5 Cell Analyzer (Bio-Rad Laboratories). Flow cytometry data was analyzed using FlowJo software.

Whole kidney mature glomeruli quantification by acid maceration

HCl maceration of kidneys from newborn mice was conducted as described previously (11-13). In brief, dissected p0 kidneys were rinsed in PBS and were digested in 6N HCl for 30 minutes at 37 °C with agitation for 15 minutes. Digested kidneys were further broken down by passing

through an 18 G needle into a 15 mL falcon tube. 1 mL PBS was used to wash the original tube twice and passed through the 18 G needle into the same 15 mL tube. Subsequently the mixture was passed through a 21 ½ G needle into a new 15 mL tube and washed with PBS using the same strategy. 5 mL of additional PBS were added to the tubes followed by 4 °C overnight incubation with agitation. After inverting the tube several times for a homogenous mixture, three separate 50 μL droplets of each kidney digestion were added to a gridded dish and the number of mature glomeruli in each droplet were counted using a dissecting microscope. Glomeruli were identified by their distinct morphology. The assay was conducted double-blinded, where the glomerular counter was blinded to the sample identity and the sample identifier was blinded to the kidney quantifications.

Collagen Zymography

12 mL of serum-free media with the addition of an EDTA-free protease inhibitor (Roche; 11836170001) was collected from *Adamts9* cKO or *Wt* littermate primary kidney cultures. Media was concentrated to ~1 mL using a 10 kDa molecular weight cutoff spin column (Thermo Fisher; 88527) by centrifugation at 4500 RPM for 15 mins. Protein concentrations of the samples were obtained using a BCA kit (Thermo Fisher; A55864). 0.3 μg of total protein from independent triplicate cultures for each genotype was run in a 10% SDS-polyacrylamide gel containing 1% gelatin (Novex, Thermo Fisher Scientific; ZY00102BOX) with using 5X Laemmli sample buffer without β-mercaptoethanol. Freshly made 1x renaturing buffer (2.7% Triton-X in ddH_2O) was added to the gel with agitation for 30 mins at RT for renaturing the samples. The gel was then incubated in 1x developing buffer (50 mM Tris HCl, 200 mM NaCl, 5mM CaCl2·2H2O, 0.006% (w/v) Brij-35 in 1L ddH_2O, pH 7.6) for 30 mins at RT with agitation. The 1x developing buffer was replaced with fresh buffer and the gel was incubated at 37 °C for additional 4 hours. The gel was washed 3x with ddH_2O for 10 mins and stained with GelCode Blue (Thermo Fisher Scientific; 24590) for 1 hour and destained using ddH_2O overnight according to manufacturer's

protocol. The washed gel were imaged using Li-COR Odyssey M scanner under white light illumination and the zymogram band intensities were quantified using ImageJ densitometry software.

Dye-quenched collagen (DQ-collagen) assay

8-chamber slides were coated with 25 µg/ml DQ collagen type 1 (compromised of a 1:11 ratio of DQ-conjugated to non-conjugated bovine collagen I, Invitrogen; D12060) for 2 hours at RT as previously described (14). A single well was left unseeded for assaying background fluorescent intensity of the DQ-collagen coating and the remaining chambers were seeded with primary kidney culture cells passaged once, from *Adamts9* cKO or *Wt* littermate controls, in 400 µl of kidney primary culture medium. After 24 hours culture at 37°C and 5% CO_2, the cell layer was washed once with PBS and fixed using freshly made 4% PFA in PBSTw (0.1%) for 10 mins at RT with agitation. The slide was washed 3x with PBSTw (0.1%) and mounted overnight using ProLong Gold medium with DAPI. Confocal images were obtained using a Leica SP8 laser scanning confocal microscope with a 63x 1.47 N.A. oil-immersion objective for capturing the DQ-collagen signal intensities of three 40x image fields from each culture. The DQ-collagen signal intensity was quantified using NIH Image J software and the background signal intensity of coated wells without any seeded cells (no cell control) were subtracted from the signal intensity measurements from the experimental groups.

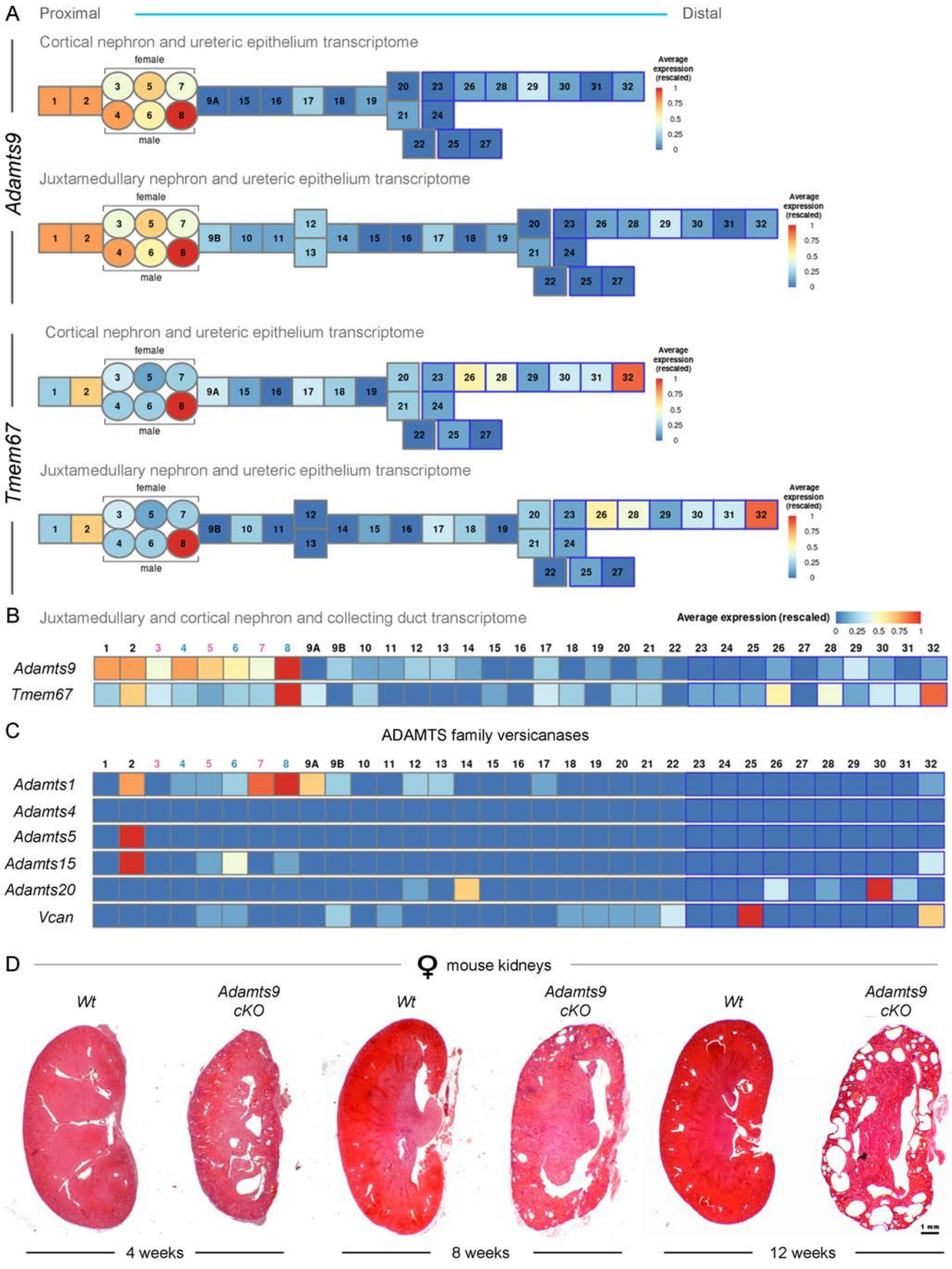
Quantification of renal histopathology and immunostaining data

Kidney area, glomeruli counts, cilia frequency, cilia length, transition zone intensity, active β-catenin intensity were all quantified using NIH Image J (FIJI). The cell counter function was used to quantify the number of glomeruli per midline kidney section and cilia frequencies. The line trace function was used to measure cilia lengths. The kidney area was quantified using the polygon tool. For quantifying transition zone marker intensities, the mean pixel intensity was measured from a ROI, specifying the signal directly above the γ-tubulin staining as previously

described (1). For active β-catenin, YAP, TAZ, pYAP and pTAZ staining, the polygon tool was used to trace the kidney tubule and measure the mean pixel intensity. All statistical tests were done using GraphPad Prism software with statistical tests and significance indicated in the figure legends.

SUPPLEMENTAL FIGURES, TABLES AND MOVIE CAPTIONS

SUPPLEMENTAL FIGURE 1



Supplemental Figure 1. Sex-specific expression patterns of *Adamts9* and *Tmem67* in the murine kidney and delayed onset of cystic kidneys in *Adamts9* cKO females.

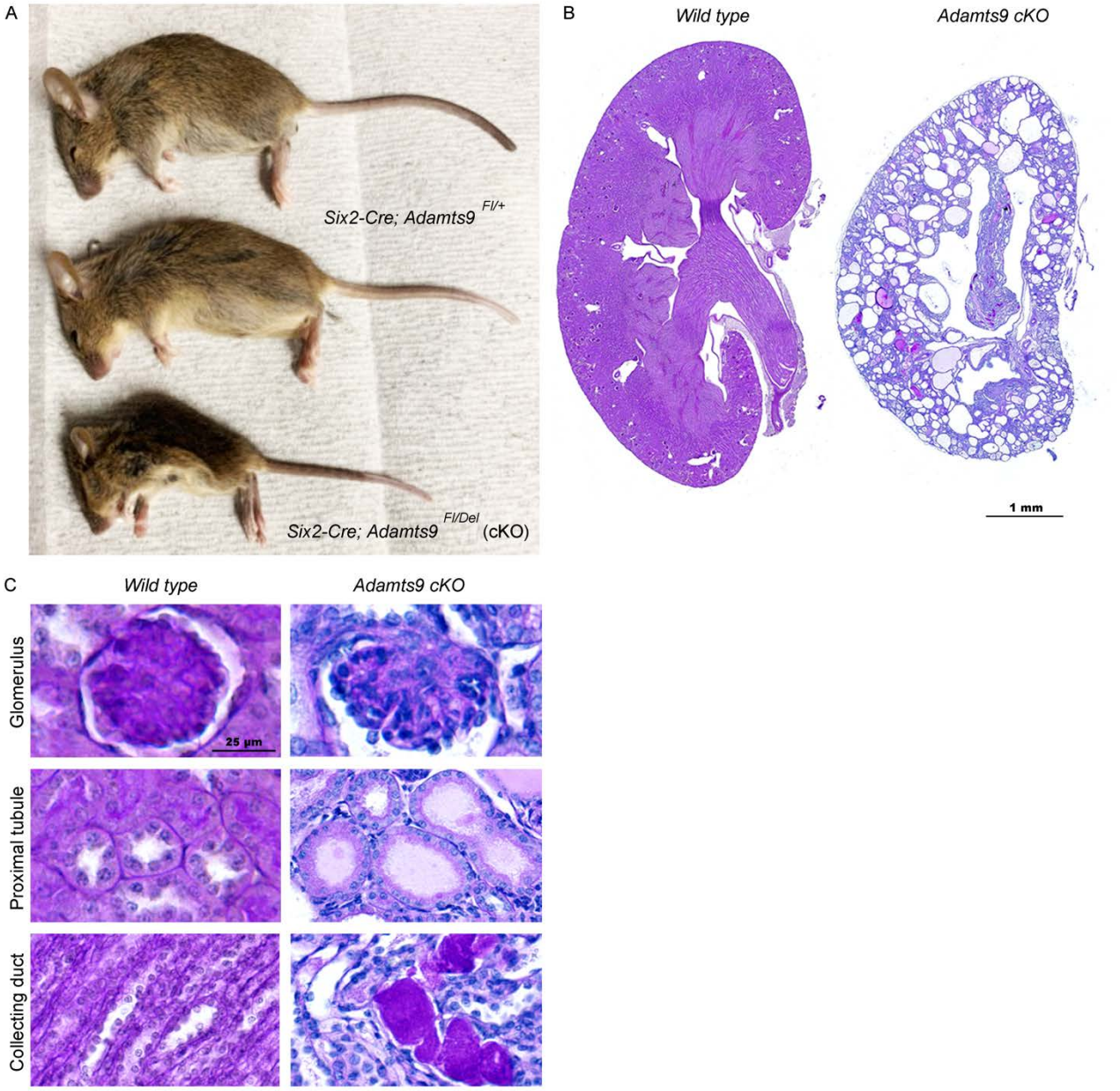
(**A-B**) Single cell RNA sequencing data for *Adamts9* and *Tmem67* in the murine kidney comparing male and female adult mouse kidneys utilizing The Kidney Cell Explorer (https://cello.shinyapps.io/kidneycellexplorer/). Ontology of cell populations pertaining to *Adamts9* and *Tmem67* expression: 1-podocytes, 2- Parietal epithelium, 3- Segment 1 of proximal tubules (female), 4- Segment 1 of proximal tubules (male), 5- Segment 2 of proximal tubules (female), 6- Segment 2 of proximal tubules (male), 7- Segment 3 of proximal tubules (female), 8- Segment 3 of proximal tubules (male), 26- Principal cell of outer medullary collecting duct, 32- Deep medullary epithelium of pelvis.

(**C**) Expression pattern of other versicanases belonging to the ADAMTS family and *Vcan* in male and female adult mouse kidneys. Ontology of key cell populations: 2- Parietal epithelium, 3- Segment 1 of proximal tubules (female), 4- Segment 1 of proximal tubules (male), 5- Segment 2 of proximal tubules (female), 6- Segment 2 of proximal tubules (male), 7- Segment 3 of proximal tubules (female), 8- Segment 3 of proximal tubules (male), 9A- Loop of Henley, thin descending limb of inner stripe of outer medulla of cortical nephron, 14- Upper loop of Henley, thin ascending limb of inner medulla of juxtamedullary nephron, 25- Intercalated type A cell of outer medullary collecting duct, 32- Deep medullary epithelium of pelvis.

(**D**) Hematoxylin and eosin staining of *Adamts9* cKO and *Wt* female littermate kidneys showing relatively slow onset of cystic pathology during 4-12 weeks of age.

Scale bar is 1 mm in **D**.

SUPPLEMENTAL FIGURE 2



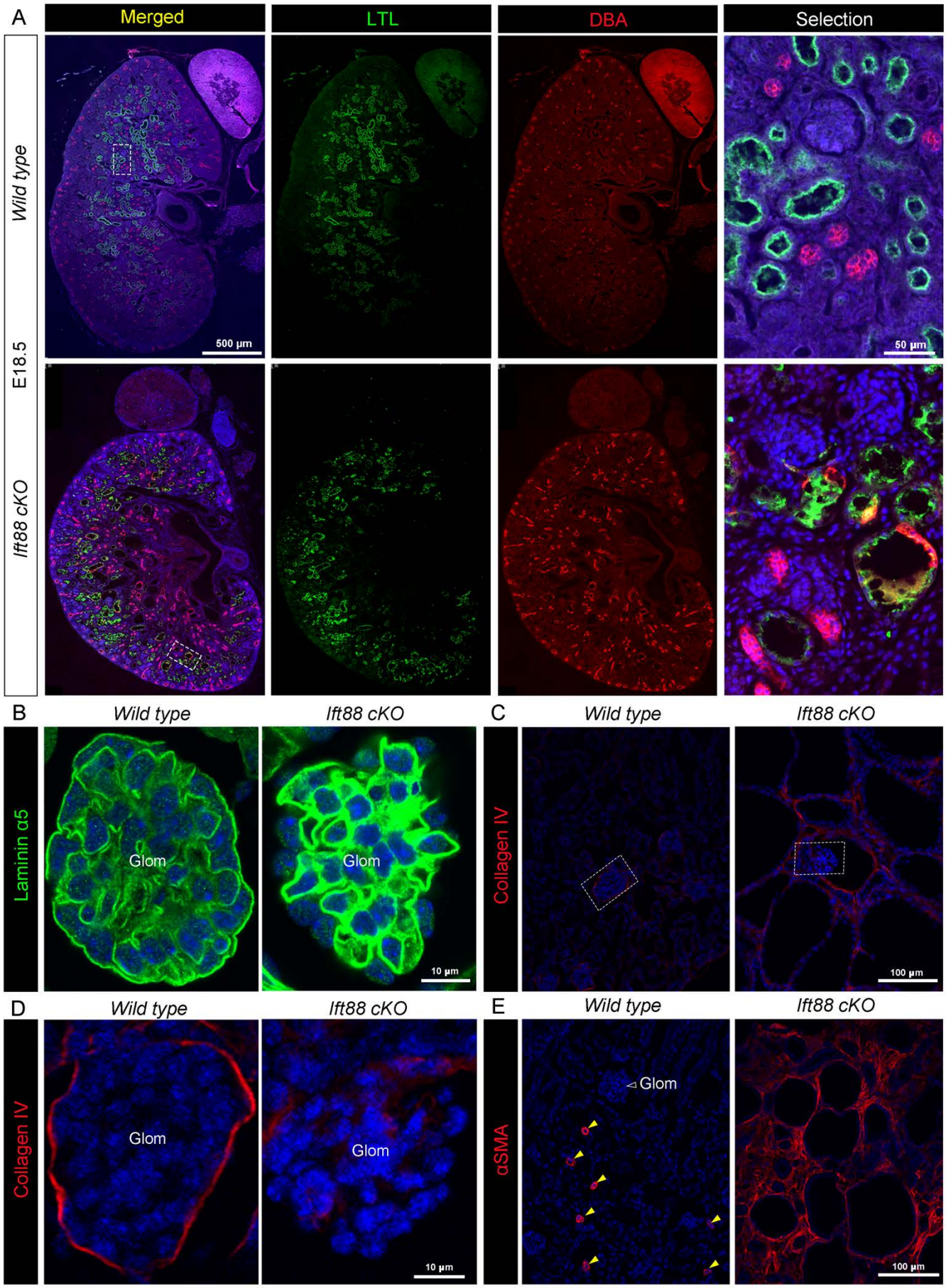
Supplemental Figure 2. End stage male *Adamts9* cKO mice and Periodic Acid-Schiff (PAS) staining of kidneys.

(**A**) *Adamts9* cKO male mice become distinguishably smaller from heterozygous littermates at 4 weeks of age.

(**B-C**) PAS staining of p21 *Wt* and *Adamts9* cKO male kidneys with magnified images of glomeruli, proximal tubules, and collecting ducts (n=3 kidneys from each genotype).

Scale bar in **B** is 1mm and 25 µm in **C**.

SUPPLEMENTAL FIGURE 3



Supplemental Figure 3. Normal embryonic nephrogenesis and ECM homeostasis defects in *Ift88* cKO kidneys .

(**A**) Male E18.5 kidneys immunostained for proximal tubules (LTL, green) and collecting ducts (DBA, red) show comparable staining levels in *Wt* and *Ift88* cKO kidneys. The boxed medullary region shown in high magnification show enlarged proximal tubule morphologies in *Ift88* cKO kidneys.

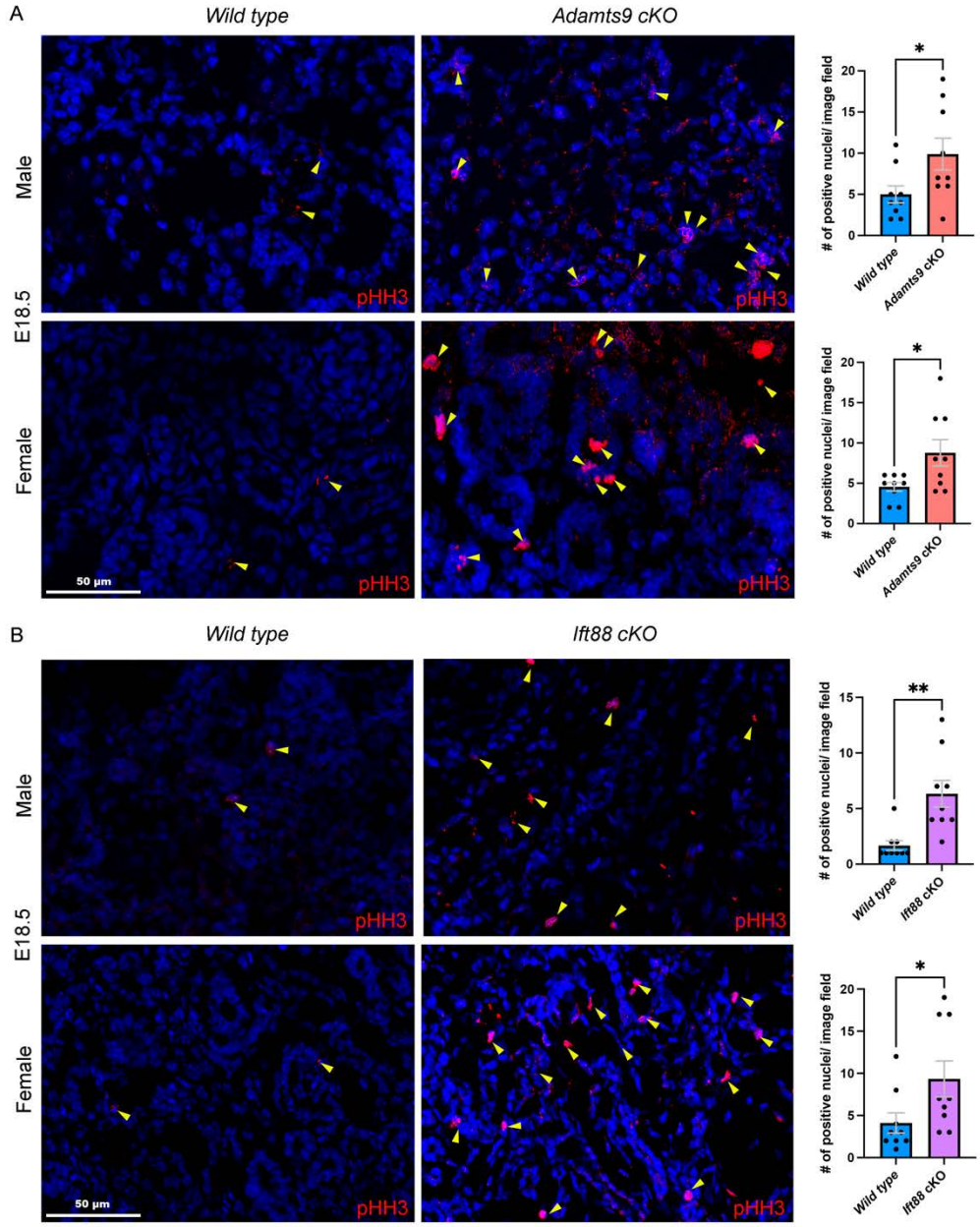
(**B**) Intense laminin α5 (green) immunostaining in *Ift88* cKO GBM in comparison to *Wt* p14 kidneys (n=3 male kidneys/ genotype).

(**C-D**) Collagen IV (red) immunostaining which is limited to the glomerulus in *Wt* kidneys did not show highly elevated staining in the *Ift88* cKO kidneys. Glomeruli marked by the white box in **B** are shown in high magnification in **C** (n=3 male kidneys/ genotype).

(**E**) α-SMA (red) immunostaining which is limited to the vasculature in *Wt* kidneys (yellow arrowheads) showed intense staining throughout the *Ift88* cKO kidneys. White open arrowhead indicates a glomerulus (n=3 male kidneys/ genotype).

Scale bars are 500 μm in **A**, 10 μm in **B** and **D,** 100 μm in **C** and **E**.

SUPPLEMENTAL FIGURE 4

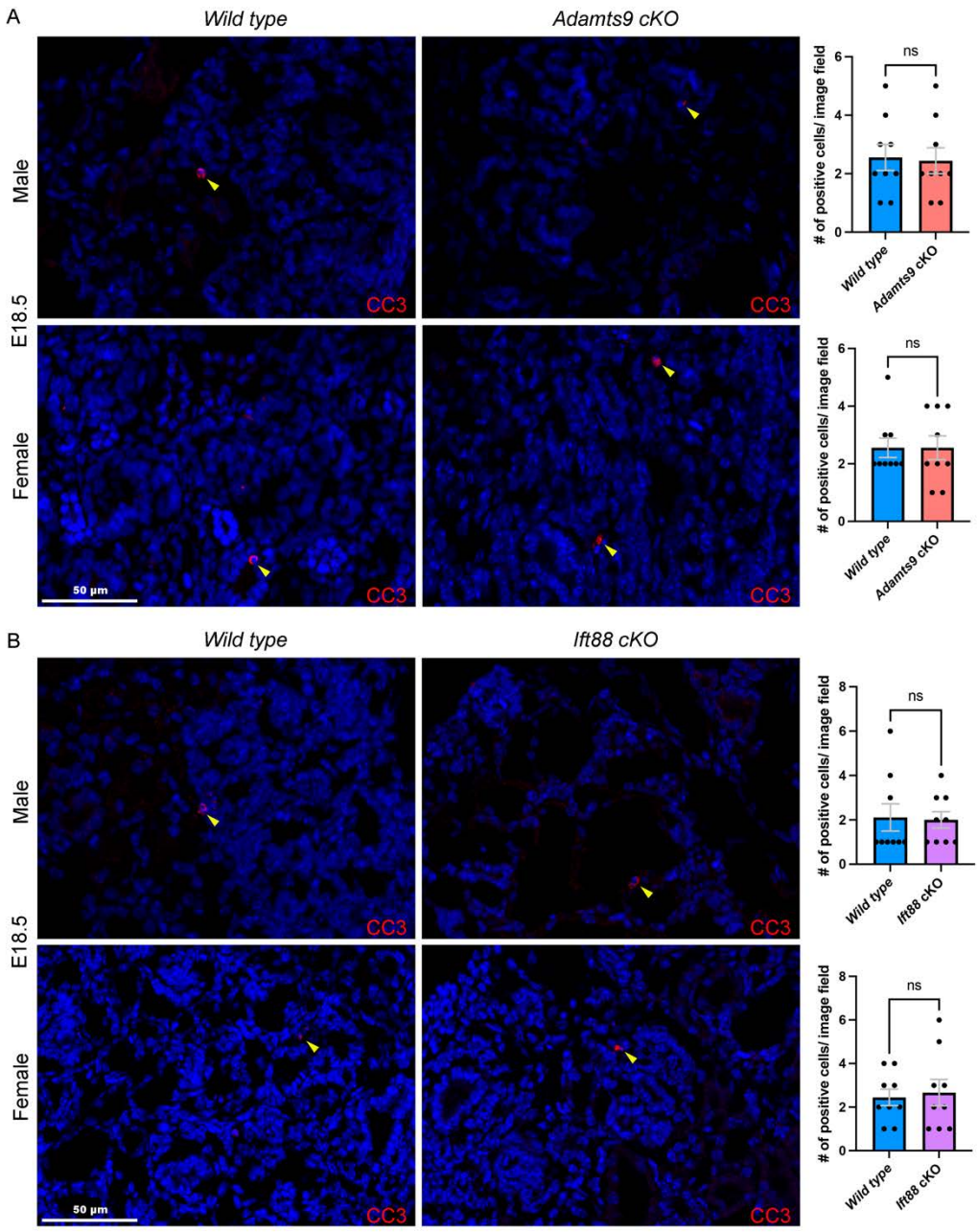


Supplemental Figure 4. Increased cell proliferation in *Adamts9* and *Ift88* cKO kidneys.

(**A-B**) Male and female *Wt*, *Adamts9* cKO and *Ift88* cKO E18.5 kidneys immunostained for the cell proliferation marker phospho Histone-H3 (pHH3, red, yellow arrowheads) shows significantly increased cell proliferation in both models compared to *Wt* kidneys (n=3 kidneys, each group).

Error bars indicate Mean ± SEM, ** indicates a *p*-value <0.01, and *<0.05 in two-tailed unpaired *t*-test. Scale bars are 50 µm in **A** and **B**.

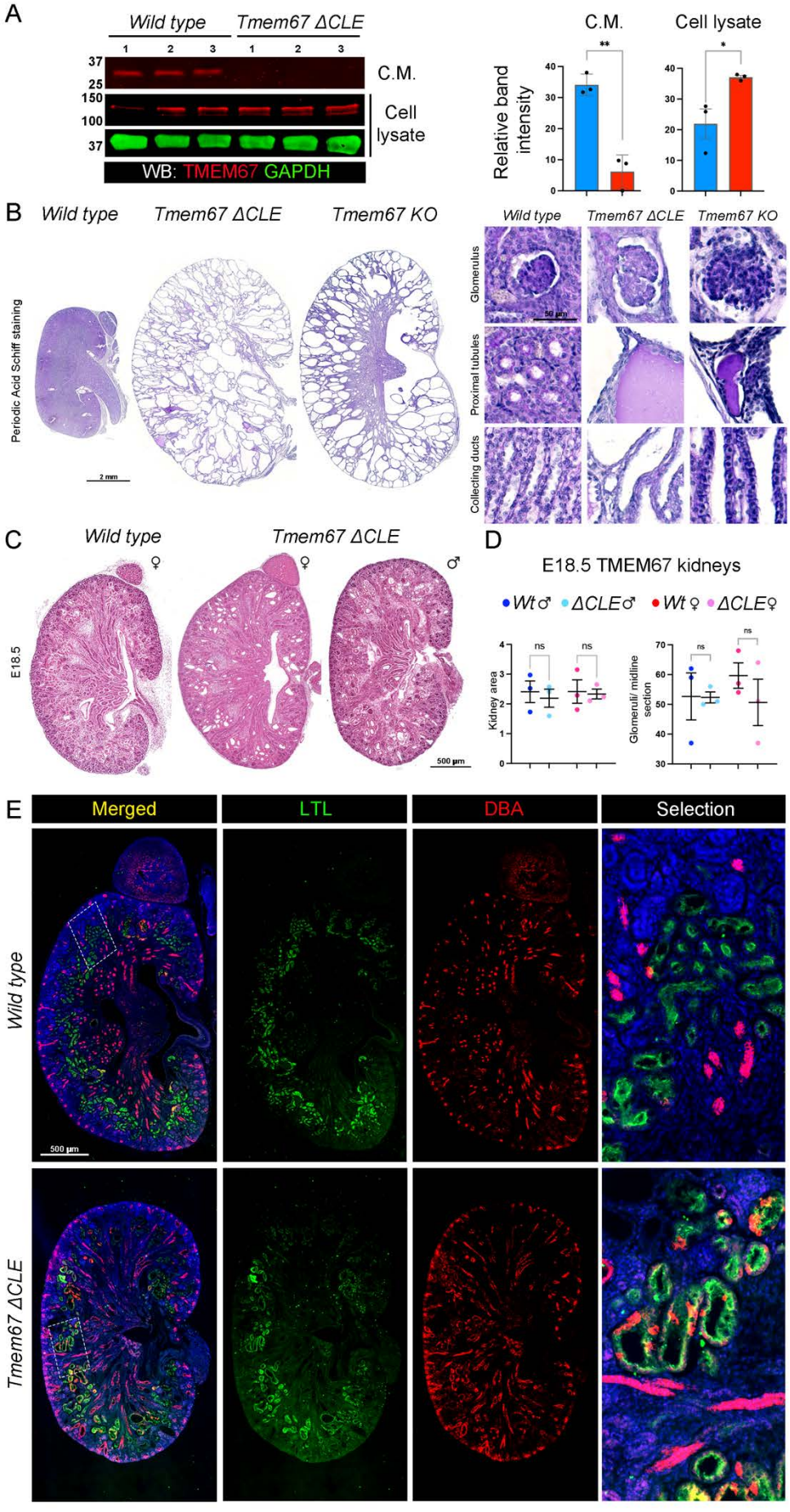
SUPPLEMENTAL FIGURE 5



Supplemental Figure 5. No significant changes in cell death in *Adamts9* and *Ift88* cKO kidneys.

(**A-B**) Male and female *Wt, Adamts9* cKO and *Ift88* cKO E18.5 kidneys immunostained for the cell death marker cleaved caspase 3 (CC3, red, yellow arrowheads) shows minimal cell death in both models (n=3 kidneys, each group). Error bars indicate Mean ± SEM, ns indicates non-significance in two-tailed unpaired *t*-test. Scale bars are 50 µm in **A** and **B**.

SUPPLEMENTAL FIGURE 6



Supplemental Figure 6. TMEM67 extracellular domain cleavage deficient mice (*Tmem67*$^{\Delta CLE/\Delta CLE}$) undergo normal embryonic kidney development.

(**A**) Western blot analysis of TMEM67 cleavage in *Wt* and *Tmem67*$^{\Delta CLE/\Delta CLE}$ primary kidney cultures show loss of the 34 kDa N-terminal fragment generated by ADAMTS9-mediated TMEM67 extracellular domain cleavage in the conditioned medium and increased full-length TMEM67 protein in the cell lysates of *Tmem67*$^{\Delta CLE/\Delta CLE}$ kidneys. (n=3 independent primary cultures, TMEM67 (red) and GAPDH (green). Error bars indicate Mean ± SEM, ** indicates a *p*-value <0.01 and * indicates a *p*-value <0.05 calculated by two-tailed unpaired *t*-test.

(**B**) PAS staining of p14 *Wt, Tmem67 KO* and *Tmem67*$^{\Delta CLE/\Delta CLE}$ with magnified images of the glomeruli, proximal tubules, and collecting ducts (n=3 male kidneys/ genotype).

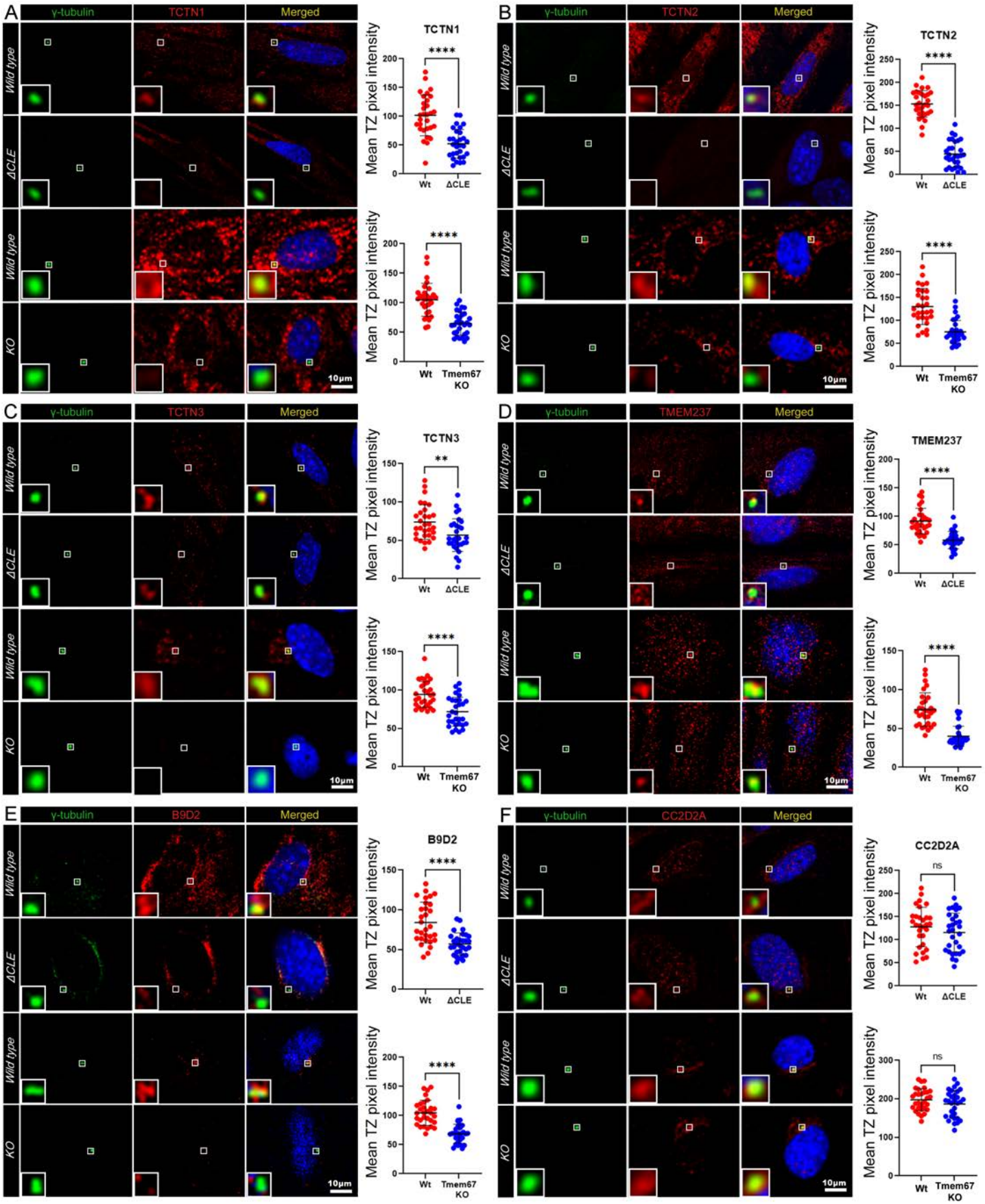
(**C**) Hematoxylin and eosin staining of E18.5 kidneys show relatively normal histology and onset of cyst formation in both male and female *Tmem67*$^{\Delta CLE/\Delta CLE}$ kidneys (n=3 kidneys/ sex/ genotype).

(**D**) Quantification of kidney area and number of glomeruli show normal nephrogenesis of E18.5 *Tmem67*$^{\Delta CLE/\Delta CLE}$ kidneys. (n=3 kidneys/ sex/ genotype). Error bars indicate Mean ± SEM, ns indicates a p-value >0.05 calculated by two-way ANOVA and Tukey's multiple comparison test.

(**E**) E18.5 kidneys immunostained for proximal tubules (LTL, green) and collecting ducts (DBA, red) show comparable staining levels in *Wt* and *Tmem67*$^{\Delta CLE/\Delta CLE}$ kidneys. The boxed medullary region shown in high magnification show enlarged proximal tubule morphologies in *Tmem67*$^{\Delta CLE/\Delta CLE}$ kidneys .

Scale bars are 2 mm and 50 μm in **B**, 500 μm in **C** and **D**.

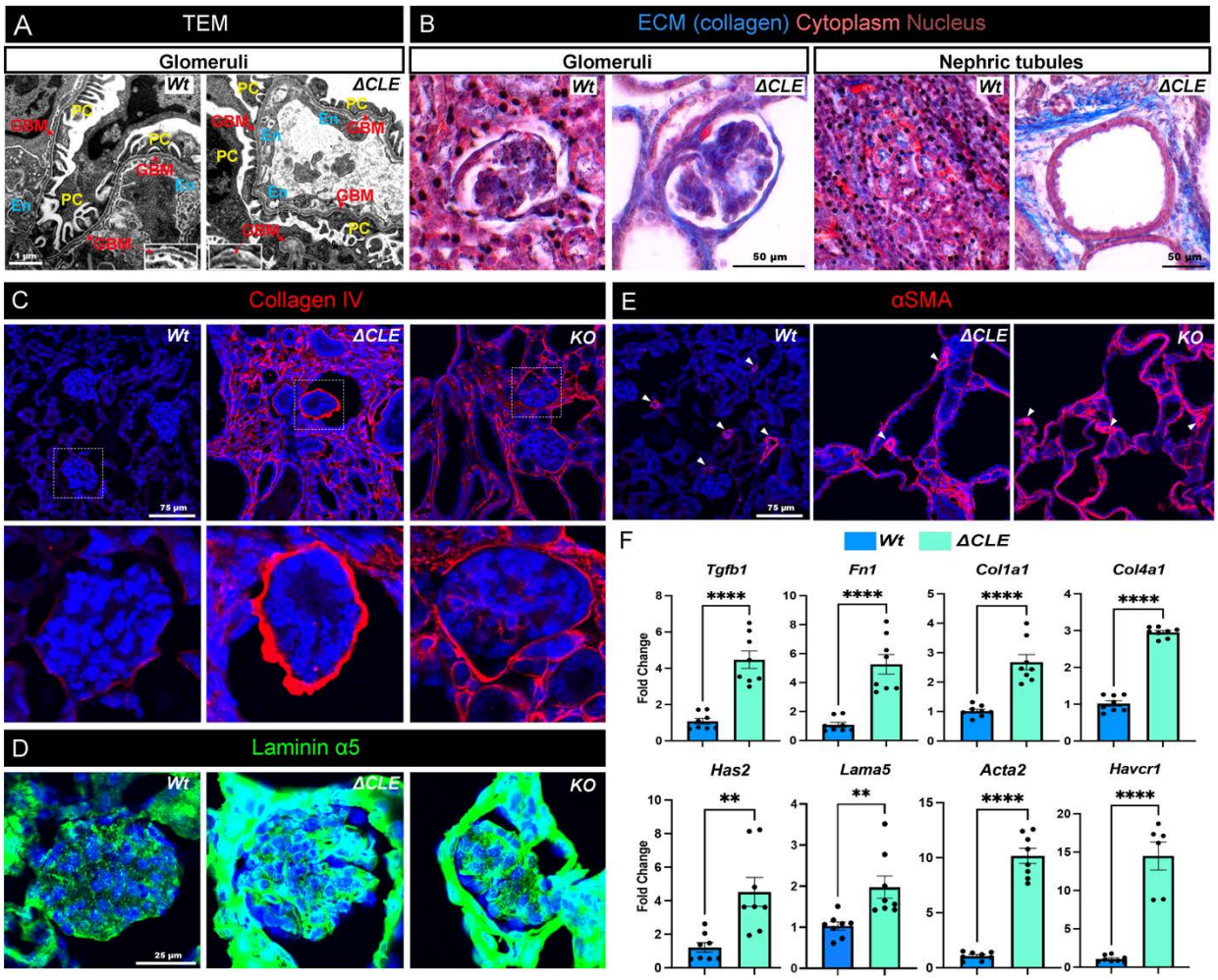
SUPPLEMENTAL FIGURE 7



Supplemental Figure 7. Los of MKS/B9 module in renal primary cilia of TMEM67 cleavage deficient and TMEM67-null kidneys.

(**A-F**) *Wt, Tmem67*$^{\Delta CLE/\Delta CLE}$, and *Tmem67* KO primary kidney cultures immunostained for γ-tubulin (green) and the TZ MKS/B9 module markers (red), show significantly lower staining for TCTN1-3, TMEM237 and B9D2 in the mutant TZs while CC2D2A is unaffected. Inserts indicate high magnification images of the TZ (n=3 experiments, 30 TZ/group). Error bars indicate Mean ± SEM, **** indicates a *p*-value <0.0001 and **<0.01 calculated by two-tailed unpaired *t*-test. Scale bars in **A-F** are 10 μm.

SUPPLEMENTAL FIGURE 8



Supplemental Figure 8. ECM homeostasis defects in *Tmem67*$^{\Delta CLE/\Delta CLE}$ and *Tmem67*-null kidneys.

(**A**) TEM images of p14 male *Wt* and *Tmem67*$^{\Delta CLE/\Delta CLE}$ kidneys show thickening of the glomerular basement membrane (GBM, red arrows). Boxed areas are shown in high magnification in the inserts. PC, podocytes; En, endothelium. (n=3 kidneys/ genotype)

(**B**) Masson's trichrome staining of p14 male *Wt* and *ΔCLE* kidneys show collagen (blue) surrounding glomeruli and cysts in the mutant kidneys (n=3 kidneys).

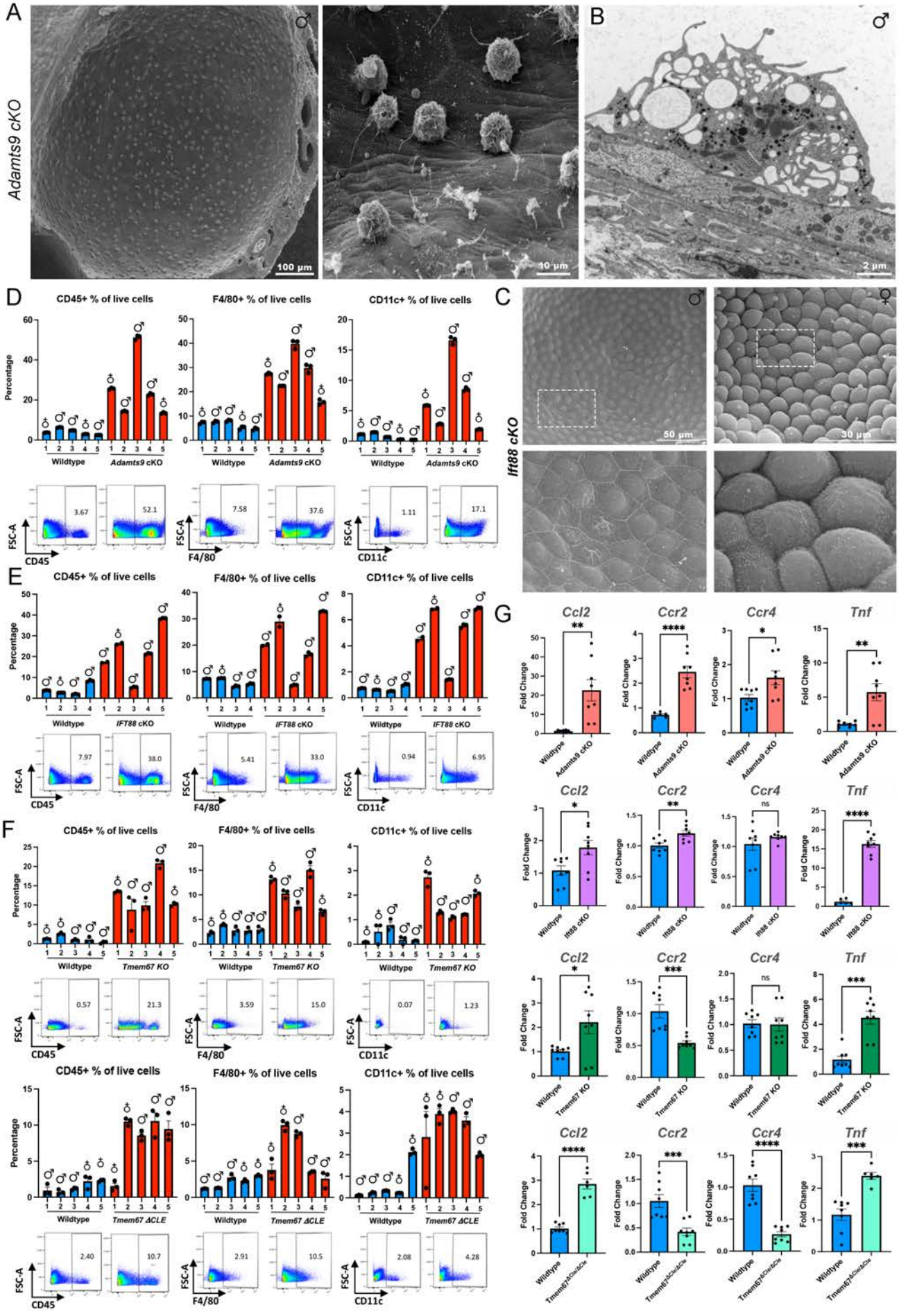
(**C**) Immunostaining for Collagen IV (red) in male p14 *Wt,* and *Tmem67 ΔCLE* and KO kidneys (n=3 kidneys/ group). Boxed area indicates a glomerulus shown in high magnification.

(**D**) Intense laminin α5 staining (green) surrounding the glomeruli of *Tmem67 ΔCLE* and *Tmem67* KO p14 male cystic kidneys (n=3 kidneys/ group).

(**E**) α-SMA staining (red), limited to the vascular capillaries (arrow heads) in male p14 *Wt* kidneys, show staining throughout *Tmem67 ΔCLE* and *Tmem67* KO cystic kidneys (n=3 kidneys/ group).

(**F**) qRT-PCR analysis of ECM-related genes (*Tgfb1, Fn1, Col1a1, Col4a1, Has2, Lama5*), kidney injury (*Havcr1*), and fibrosis (*Acta2*) markers of p14 male *Wt* and *Tmem67*$^{\Delta CLE/\Delta CLE}$ kidneys show increased transcription (n=4 kidneys/ genotype). Error bars indicate Mean ± SEM, **** indicates a p-value <0.0001,***<0.001, and **<0.01 calculated by two-tailed unpaired *t*-test. Scale bar in **A** is 1 μm, 50 μm in **B**, 75 μm in **C** and **E**, and 25 μm in **D**.

SUPPLEMENTAL FIGURE 9



Supplemental Figure 9. Macrophage infiltration in *Adamts9* cKO cystic lumens and immune response of cystic kidney models.

(**A-B**) SEM (**A**), and TEM (**B**) images of p21 male *Adamts9* cKO kidneys showing large numbers of macrophages residing in their cystic lumens (n=3 kidneys). Left image in **A** shows a single cystic lumen from freeze-fracture SEM and the right image showed a high magnification of the cystic surface. TEM image in **B** shows morphology of the macrophages residing in the cystic lumen with many membrane protrusions, vacuoles and lysosomes.

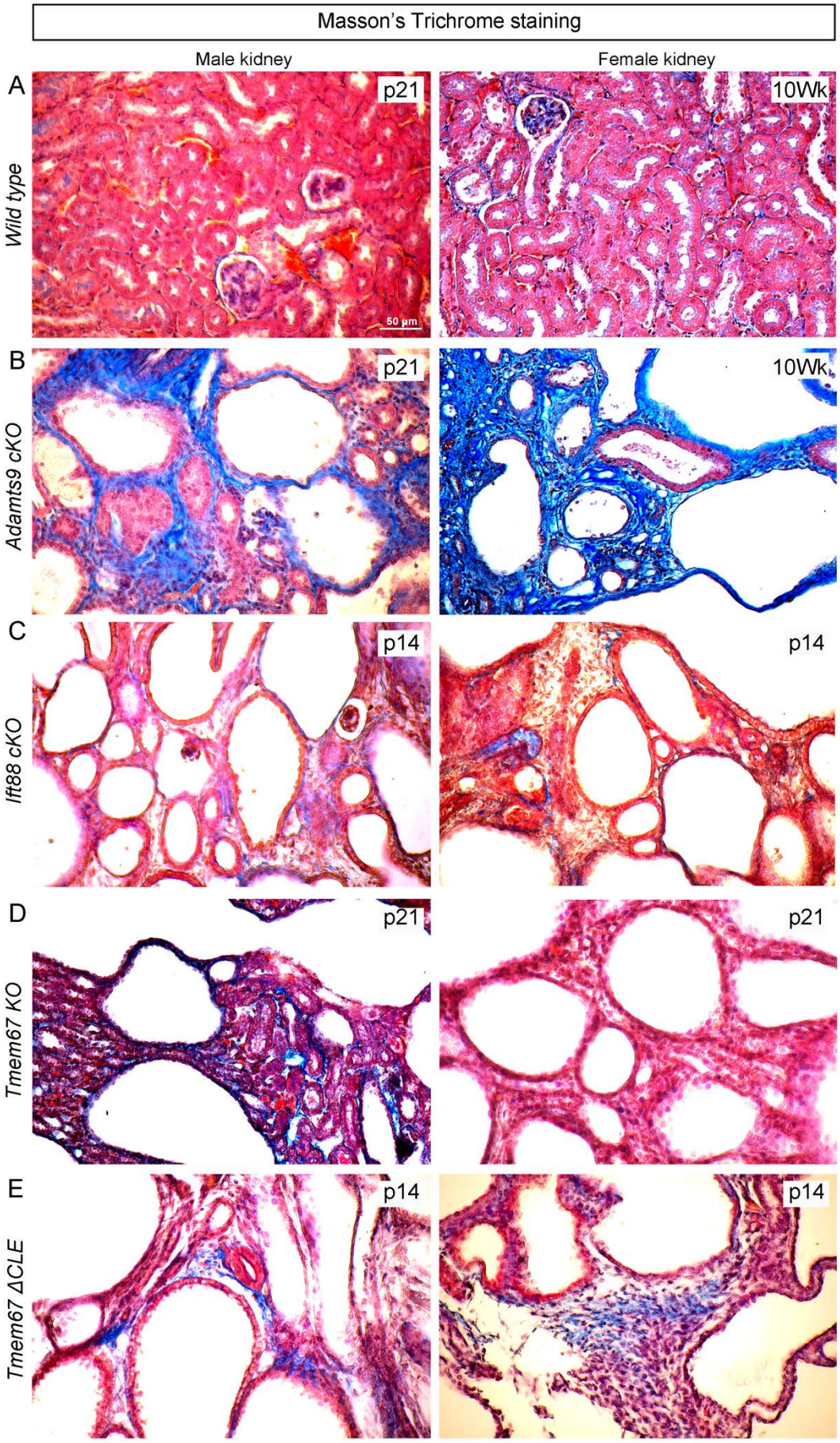
(**C**) Freeze-fracture SEM images of p14 male and female *Ift88* cKO kidney cysts which did not show any macrophages residing in their cystic lumens (n=3 kidneys).

(**D-F**) Flow cytometry analysis of immune cells present in whole kidneys of *Adamts9* cKO (**D**), *Ift88* cKO (**E**), *Tmem67* KO and *Tmem67*$^{\Delta CLE/\Delta CLE}$ kidneys (**F**), in comparison to littermate kidneys show high levels of CD45+, F4/80+ and CD11c+ cells in cystic kidneys from both sexes with the *Adamts9* cKO kidneys showing the highest percentages for each group (n=39 mice/ kidneys). Blue boxes mark *Wt* littermates and red boxes mark cystic kidneys. Error bars in each column indicate Mean ± SEM of 2-3 technical replicates of each kidney. Scatter plots of a representee male kidney is shown for each genetic group.

(**G**) qRT-PCR analysis for expression levels of *Ccl2, Ccr2, Ccr4* and *Tnf* in male cystic kidneys of *Adamts9* cKO, *Ift88* cKO, *Tmem67* KO and *Tmem67 ΔCLE* kidneys show transcriptional upregulation of immune activity in the cystic kidneys (n=4 kidneys/ genotype). Error bars indicate Mean ± SEM, **** indicates a p-value <0.0001, ***<0.001, **<0.01, and *<0.05 calculated by two-tailed unpaired *t*-test.

Scale bar in **A** is 100 μm, 2 μm in **B,** 50 μm and 30 μm in **C**.

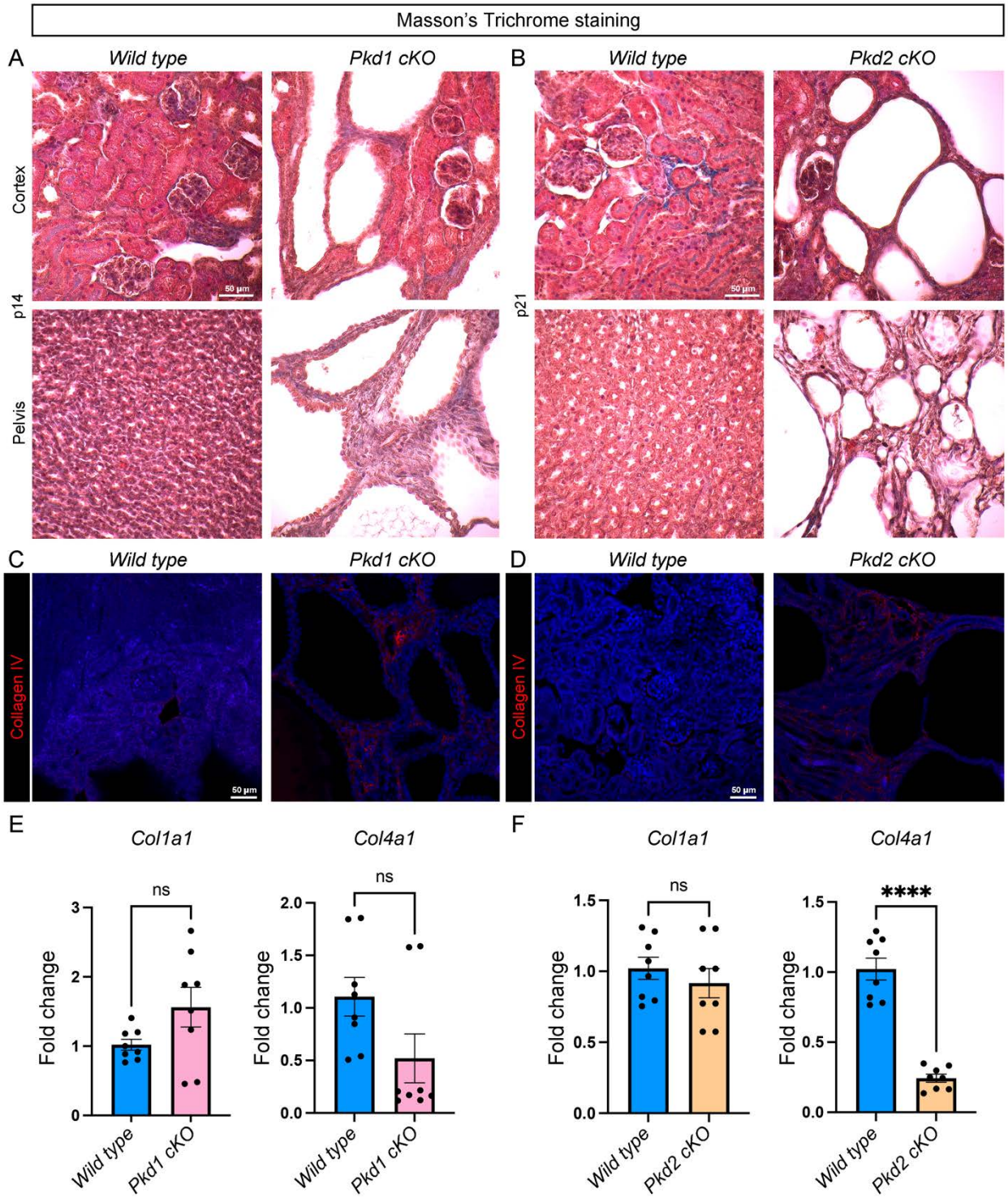
SUPPLEMENTAL FIGURE 10



Supplemental Figure 10. Comparably higher levels of collagen accumulation in *Adamts9* cKO cystic kidneys.

(**A-D**) Low magnification images comparing Masson's trichrome stained kidney sections of *Wt* (**A**), *Adamts9* cKO (**B**), *Ift88* cKO (**C**), *Tmem67* KO (**D**), and *Tmem67 ΔCLE* kidneys (**E**), show distinctly higher levels of collagen (blue staining) present throughout the cystic kidneys of both male (p21) and female (10 week old) *Adamts9* cKO kidneys which may be suppressing the rapid enlargement of *Adamts9* cKO cystic kidneys in comparison to the other cystic kidney models.

SUPPLEMENTAL FIGURE 11



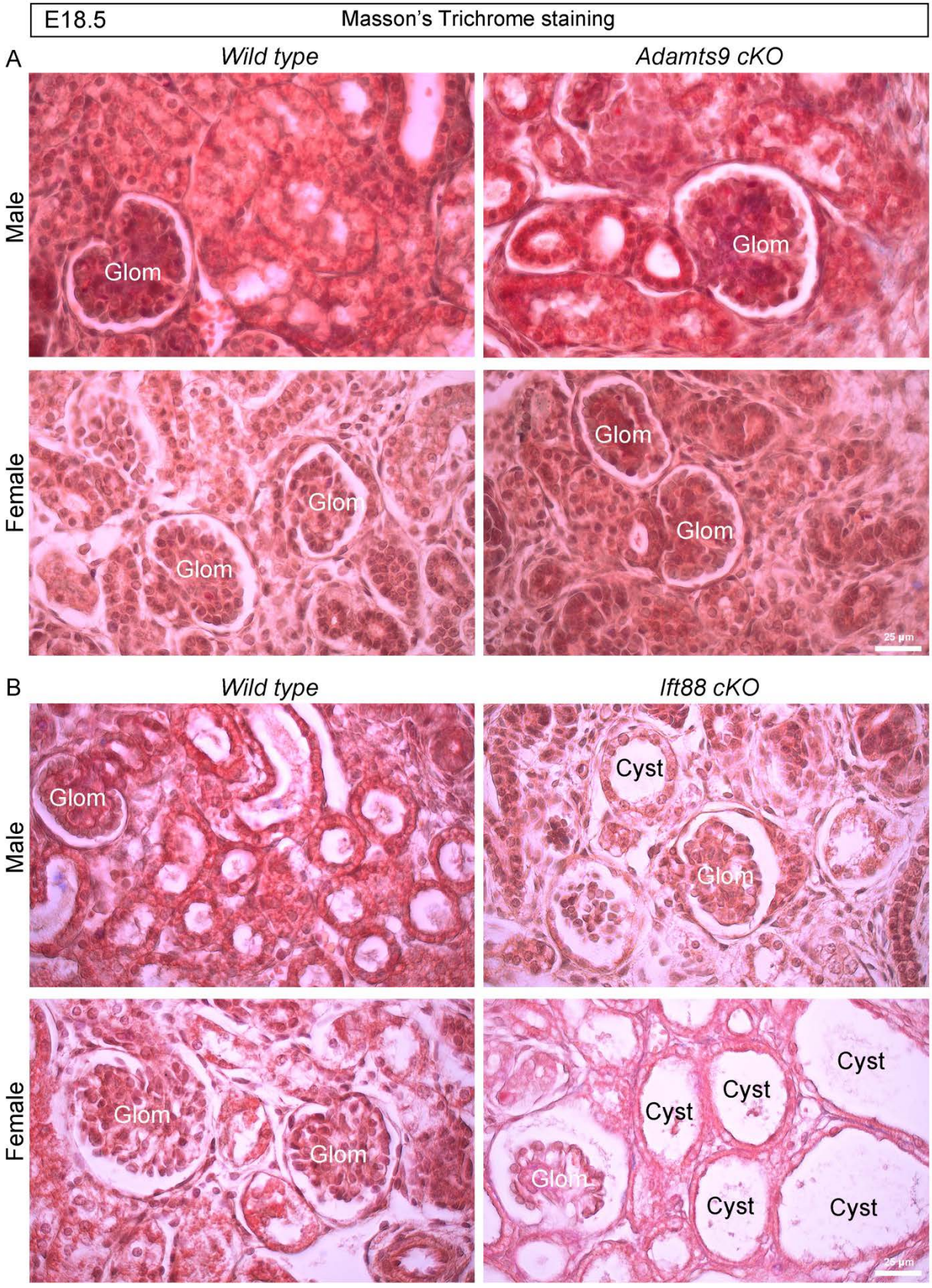
Supplemental Figure 11. Comparably low levels of collagen in end stage *Pkd1 and Pkd2* cKO cystic kidneys.

(**A-B**) Low magnification images comparing Masson's trichrome stained kidney sections of male *Wt* and *Pkd1* cKO *(Hoxb7-Cre; Pkd1*$^{Fl/Fl}$) kidneys at p14 (**A**), and *Pkd2* cKO *(Rosa26-Cre*^{ERT}*; Pkd2*$^{Fl/Fl}$) kidneys at p21 (**B**), show very minimal levels of collagen (blue staining) present in the *Pkd* cKO cystic kidney models (n=5 male kidneys from each group).

(**C-D**) Collagen-IV immunostaining show very low level of little staining in *Pkd1* and *Pkd2* cKO kidneys (n=5 male kidneys from each group).

(**E-F**) qRT-PCR analysis shows no significant changes in *Col1a1* transcription while *Col4a1* is down regulated in *Pkd1* and *Pkd2* cKO kidneys (n=4 male kidneys from each group). Error bars indicate Mean ± SEM, **** indicates a p-value <0.0001calculated by two-tailed unpaired *t*-test. Scale bars in **A-D** are 50 μm.

SUPPLEMENTAL FIGURE 12

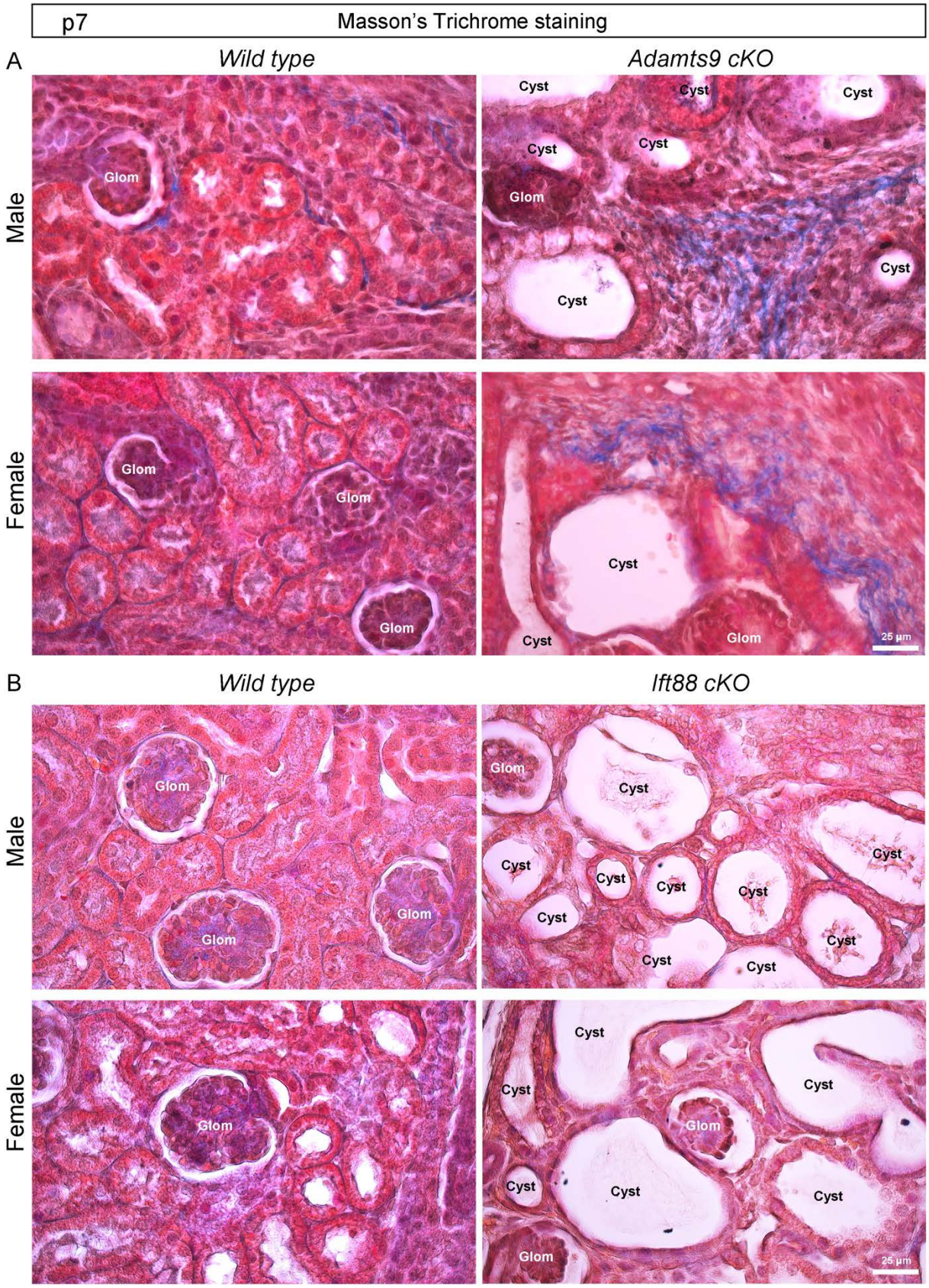


Supplemental Figure 12. Embryonic *Adamts9* and *Ift88* cKO kidneys do not show collagen accumulation.

(**A-B**) Masson's trichrome stained sections of E18.5 male and female *Wt*, *Adamts9* and *Ift88* cKO kidneys do not show any collagen accumulation at the end of gestation in either model or in *Wt* kidneys (n=3/ sex/genotype).

Scale bars in **A-B** are 25 μm.

SUPPLEMENTAL FIGURE 13

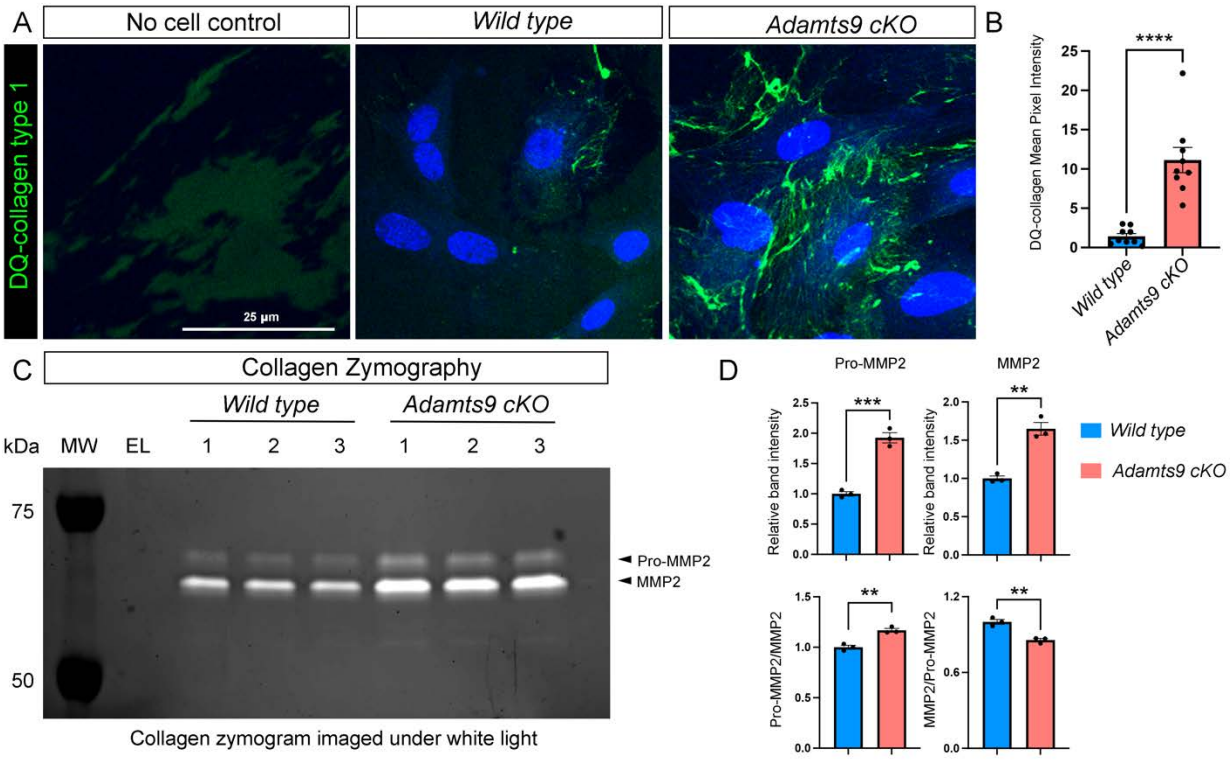


Supplemental Figure 13. Distinct interstitial collagen accumulations in *Adamts9* but not *Ift88* cKO kidneys by one week of age.

(**A-B**) Masson's trichrome stained sections of 1-week old male and female *Wt*, *Adamts9* and *Ift88* cKO kidneys show distinct interstitial collagen depositions surrounding the *Adamts9* cKO cysts but not in the *Ift88* cKO kidneys or *Wt* (n=3/ sex/genotype).

Scale bars in **A-B** are 25 μm.

SUPPLEMENTAL FIGURE 14



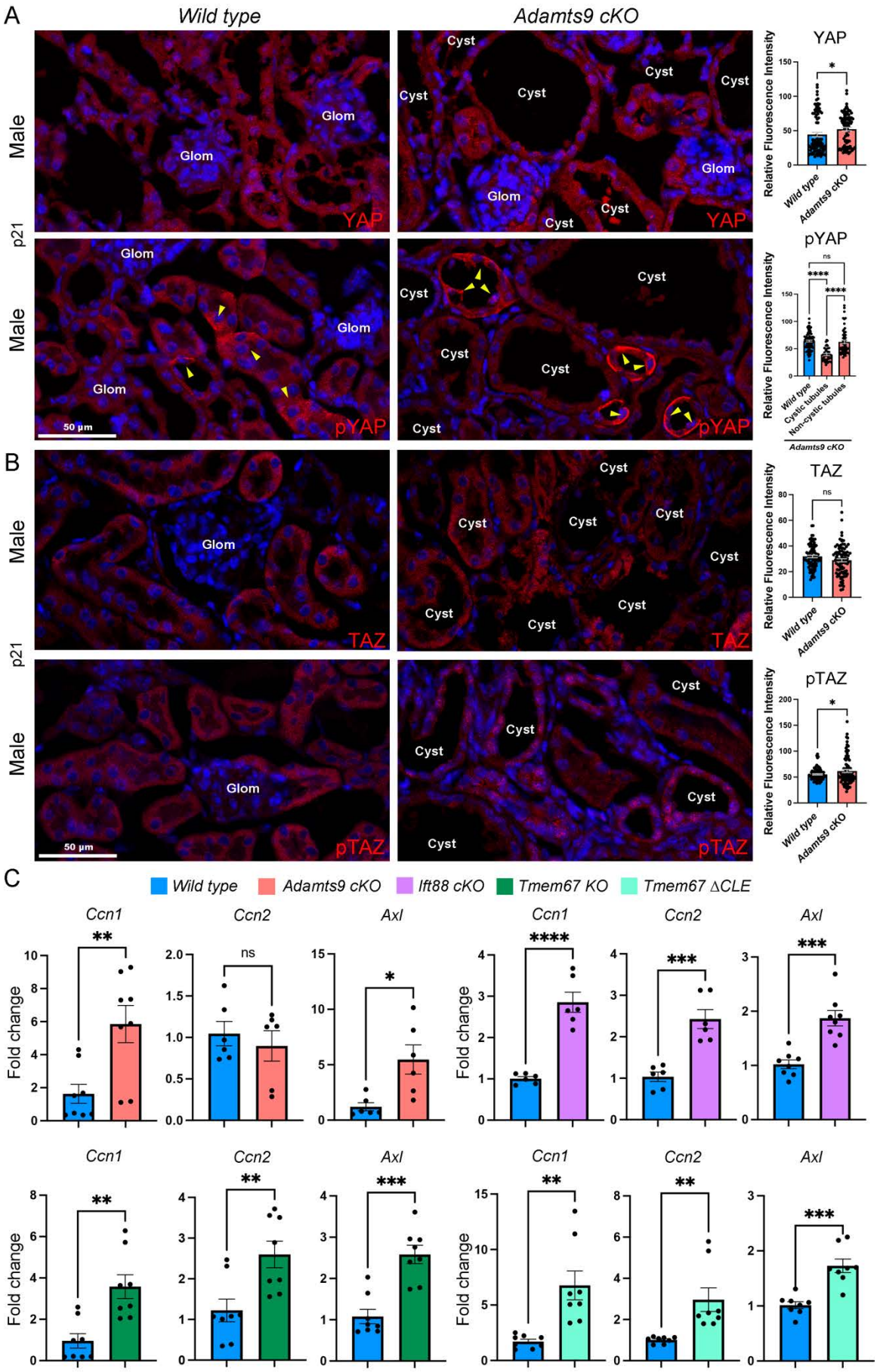
Supplemental Figure 14. Increased cell surface MT_1-MMP activity in *Adamts9* cKO kidneys.

(**A-B**) p21 male *Adamts9* cKO or *Wt* littermate control kidney primary cultures grown in DQ-collagen (dye-quenched) type-1coated chamber slides show significantly more Fluorescein DQ-collagen signal (green) surrounding the *Adamts9* cKO cells (n=3 independent cultures). No cell control indicates a coated culture well without any cells seeded. Error bars indicate Mean ± SEM, **** indicates a p-value<0.0001 by two-tailed unpaired *t*-test.

(**C-D**) Collagen zymography of the conditioned medium of p21 male *Adamts9* cKO or *Wt* littermate control kidney primary cultures show increased MMP2 released by *Adamts9* cKO kidneys. M.W., molecular weight; E.L., empty lane. Relative band intensities are normalized to the mean value of the *Wt* bands in **D**. Error bars indicate Mean ± SEM, *** indicates a p-value<0.001, **<0.01 calculated by two-tailed unpaired *t*-test.

Scale bar in **A** is 25 µm.

SUPPLEMENTAL FIGURE 15



Supplemental Figure 15. YAP/TAZ signaling in *Adamts9* cKO cystic renal tubular epithelium and the other cystic kidney models

(**A**) YAP and phospho-YAP (pYAP) immunostaining of p21 male *Wt* and *Adamts9* cKO kidneys (n=3 kidneys/ genotype, 30 tubules/ kidney). Error bars indicate Mean ± SEM, * indicates a p-value<0.05 calculated by two-tailed unpaired *t*-test for YAP and **** indicates a p-value<0.0001 calculated by two-way ANOVA and Tukey's multiple comparison test for pYAP.

(**B**) TAZ and phospho-TAZ (pTAZ) immunostaining of p21 male *Wt* and *Adamts9* cKO kidneys (n=3 kidneys/ genotype, 30 tubules/ kidney). Error bars indicate Mean ± SEM, ns indicates non significance and * indicates a p-value<0.05 calculated by two-tailed unpaired *t*-test.

(**C**) qRT-PCR analysis for expression levels of *Ccn1, Ccn2,* and *Axl* in terminal stage male cystic kidneys of *Adamts9* cKO, *Ift88* cKO, *Tmem67* KO and *Tmem67 ΔCLE* kidneys show transcriptional upregulation of the YAP/TAZ signaling target genes (n=3-4 kidneys/ genotype). Error bars indicate Mean ± SEM, **** indicates a p-value <0.0001, ***<0.001, **<0.01, and *<0.05 calculated by two-tailed unpaired *t*-test.

Scale bars in **A** and **B** are 50 μm.

Supplemental Table 1: Mouse genotyping primers

Mouse allele/ primer	Sequence (5'-3')
Six2-Cre-F	5'-ATGCTCATCCGGAGTTCCGTATG-3'
Six2-Cre-R	5'-CACCTTGTCGCCTTGCGTATAA-3'
Adamts9$^{Fl/+}$-F	5'-TTCAGAGTAGATTTGGCAGGA-3'
Adamts9$^{Fl/+}$-R	5'-ATGTTGAGCCAAGAAAGTTC-3'
Adamts9$^{Del/+}$-F	5'-GTAAGCACCAGCTAACACAG-3'
Adamts9$^{Del/+}$-R	5'-CTCATAATGGCCCTGCTCT-3'
Ift88$^{Fl/+}$-F	5'-GACCACCTTTTTAGCCTCCTG-3'
Ift88$^{Fl/+}$-R	5'-AGGGAAGGGACTTAGGAATGA-3'
Tmem67$^{+/-}$-F	5'-AGCATGTAAGGAAAGATGTTGAG-3'
Tmem67$^{+/-}$-R	5'-CCTATGCAATGGAGAGTGTACTT-3'
Tmem67$^{\Delta CLE/+}$-F	5'-ATCACCTAATGCAAACGTCTCTCT-3'
Tmem67$^{\Delta CLE/+}$-R	5'-ATTTTAGGGTTTAGGAGCAGCACT-3'
Ksp-Cre-F	5'-GCAGATCTGGCTCTCCAAAG-3'
Ksp-Cre-R	5'-AGGCAAATTTTGGTGTACGG-3'
Vcan$^{AA/+}$-F	5'-TTGCAGCTCACAGCATCA-3'
Vcan$^{AA/+}$-R	5'-TACACACAAAGAGGATTT-3'
Vcan$^{Fl/+}$-F	5'-GGGGCGGTCATAGCAAGCCC-3'
Vcan$^{Fl/+}$-R	5'-AACAGCCCTCTCGGGGAGCC-3'
Pkd1$^{Fl/+}$-F	5'-CCTGCCTTGCTCTACTTTCC-3'
Pkd1$^{Fl/+}$-R	5'-AGGGCTTTTCTTGCTGGTCT-3'
Pkd2$^{Fl/+}$-F	5'-GGGGTTTCCTATGAAGAGTTCCAAG-3'
Pkd2$^{Fl/+}$-R	5'-CTGACAGGCACCTACAGAACAGTG-3'
Cre-F	5'-GCGGTCTGGCAGTAAAAACTATC-3'
Cre-R	5'-GTGAAACAGCATTGCTGTCACTT-3'

Supplemental Table 2: Primers utilized in site directed mutagenesis of *ADAMTS9*

Construct	Sequence (5'-3')
ADAMTS9-S636F-F	5'-GAAATTTAAGTTTTGCAACACGGAG-3'
ADAMTS9-S636F-R	5'-ATTCTACGTCCTACACAG-3'
ADAMTS9-R647Q-F	5'-CAAGCAGAAGCAGGACTTCCGAG-3'
ADAMTS9-R647Q-R	5'-AGACATGGCTCCGTG-3'
ADAMTS9-C1024-F	5'-AAGGGCTATTTAAGTCAATACCCGAAATG-3'
ADAMTS9-C1024-R	5'-CTCCTCTGGGTCCCAC-3'
ADAMTS9-R1203W-F	5'-GAAAGGTACCTGGATGAGATACG-3'
ADAMTS9-R1203W-R	5'-CCACAAGTGGCTGAC-3'
ADAMTS9-P1665S-F	5'-CACGCAGCCCAGCAGTGTTCACC-3'
ADAMTS9-P1665S-R	5'-CCTGGGCAGTTGATGG-3'
ADAMTS9-S1826N-F	5'-TGGGTTTTCCAACTTTCAGAAAATCAGAATAGAC-3'
ADAMTS9-S1826N-R	5'-GCGGCCGTGTAATCC-3'

Supplemental Table 3: qRT-PCR primers used in this study

Gene	Sequence (5'-3')	Species
18s-F	5'-TTGACGGAAGGGCACCACCAG-3'	Mouse
18s-R	5'-GCAACCACCACCCACGGAATCG-3'	Mouse
Tgfb1-F	5'-CTGCTGACCCCCACTGATAC-3'	Mouse
Tgfb1-R	5'-AGCCCTGTATTCCGTCTCCT-3'	Mouse
Fn1-F	5'-CCCTATCTCTGATACCGTTGTCC-3'	Mouse
Fn1-R	5'-TGCCGCAACTACTGTGATTCGG-3'	Mouse
Col1a1-F	5'-CCTCAGGGTATTGCTGGACAAC-3'	Mouse
Col1a1-R	5'-CAGAAGGACCTTGTTTGCCAGG-3'	Mouse
Col4a1-F	5'-ATGGCTTGCCTGGAGAGATAGG-3'	Mouse
Col4a1-R	5'-TGGTTGCCCTTTGAGTCCTGGA-3'	Mouse
Has2-F	5'-CATCTGTGGAGATGGTGAAGGTC-3'	Mouse
Has2-R	5'-AGCCATCCAGTATCTCACGCTG-3'	Mouse
Lama5-F	5'-ACCCAAGGACCCACCTGTAG-3'	Mouse
Lama5-R	5'-TCATGTGTGCGTAGCCTCTC-3'	Mouse
Acta2-F	5'-GTCCCAGACATCAGGGAGTAA-3'	Mouse
Acta2-R	5'-TCGGATACTTCAGCGTCAGGA-3'	Mouse
Havcr1-F	5'-CTGGAATGGCACTGTGACATCC-3'	Mouse
Havcr1-R	5'-GCGATGCCAACATAGAAGCCC-3'	Mouse
Ccl2-F	5'-TCTGGGCCTGCTGTTCACA-3'	Mouse
Ccl2-R	5'-GGATCATCTTGCTGGTGAATGA-3'	Mouse
Ccr2-F	5'-GCTGTGTTTGCCTCTCTACCAG-3'	Mouse
Ccr2-R	5'-CAAGTAGAGGCAGGATCAGGCT-3'	Mouse
Ccr4-F	5'-GGACTAGGTCTGTGCAAGATCG-3'	Mouse
Ccr4-R	5'-TGCCTTCAAGGAGAATACCGCG-3'	Mouse
Tnf-α-F	5'-ACCCTCACACTCAGATCATCTTC-3'	Mouse
Tnf-α-R	5'-TGGTGGTTTGCTACGACGT-3'	Mouse
Hadh-F	5'-TTCCAGAGGCTGGACAAGTTCG-3'	Mouse
Hadh-R	5'-GCCAGCAAATCGGTCTTGTCTG-3'	Mouse
Lcor-F	5'-GACTCACCTCTGGACCTTAACTG-3'	Mouse
Lcor-R	5'-CTGGAGAATGGCTCAGGGAAGT-3'	Mouse
Plod2-F	5'-CATCCGAGAGTTCATTGCTCCAG-3'	Mouse
Plod2-R	5'-GCGCTGTCTTTCAGGTGAGTAC-3'	Mouse
Ccn1-F	5'-GTGAAGTGCGTCCTTGTGGACA-3'	Mouse
Ccn1-R	5'-CTTGACACTGGAGCATCCTGCA-3'	Mouse
Ccn2-F	5'-TGCGAAGCTGACCTGGAGGAAA-3'	Mouse
Ccn2-R	5'-CCGCAGAACTTAGCCCTGTATG-3'	Mouse
Axl-F	5'-GGTGTTTGAGCCAACCGTGGAA-3'	Mouse
Axl-R	5'-GCCACCTTATGCCGATCTACCA-3'	Mouse

Supplemental Table 4: Key Resource Table

REAGENT or RESOURCE	SOURCE	IDENTIFIER
Antibodies and Lectins		
Rabbit anti-Collagen IV (IF, 1:400)	Thermo Fisher Scientific	AB_11183330
Mouse anti-α-Smooth Muscle Cy3 Conjugated (IF, 1:800)	Sigma-Aldrich	AB_476856
Rabbit anti- Laminin α5 (IF, 1:200)	Kerafast	Cat#EWL005
Rat anti-ARL13B (IF, 1:400)	BiCell Scientific	AB_3170226
Rabbit anti-FGFT1OP (FOP) (IF, 1:400)	Proteintech	AB_2103362
Mouse anti-γ tubulin (IF, 1:200)	Sigma-Aldrich	AB_297920
Rabbit anti-TCTN1 (IF, 1:400)	Proteintech	AB_10644442
Rabbit anti-TCTN2 (IF, 1:400)	Proteintech	AB_2202406
Rabbit anti-TCTN3 (IF, 1:400)	Proteintech	AB_10638442
Rabbit anti-TMEM237 (IF, 1:400)	Thermo Fisher Scientific	AB_2648665
Rabbit anti-B9D2 (IF, 1:400)	Proteintech	AB_2878981
Rabbit anti-CC2D2A (IF, 1:400)	Proteintech	AB_2879063
Rabbit anti-MKS3 (TMEM67) (WB, 1:1000; IF, 1:500)	Proteintech	AB_10638441
Rabbit anti-TMEM67-C (IF, 1:400)	Colin Jonson Lab	N/A
Mouse anti-GAPDH (WB, 1:1000)	Millipore	AB_2107426
Rabbit active β-catenin (IF, 1:200)	Cell Signaling Technology	AB_11127203
Lotus Tetragonolobus Lectin (LTL) Fluorescein labelled (IF, 1:200)	Vector Laboratories	AB_2336559
Dolichos Biflorus Agglutinin (DBA) Rhodamine conjugated (IF, 1:200)	Vector Laboratories	AB_2336396
Tmem67-C (IF, 1:400)	Abdelhamed et al., Hum Mol Genet (2013)	N/A
Rabbit anti-acetylated α-tubulin (IF, 1:500)	Cell Signaling Technology	AB_10544694
Mouse anti-Calbindin D28K (IF, 1:200)	Thermo Fisher Scientific	AB_2802627
Mouse anti-Meis1/2/3 (IF, 1:200)	Active Motif	AB_2750570

Goat anti-Mouse Alexa Fluor 488 (IF, 1:500)	Thermo Fisher Scientific	AB_2536161
Goat anti-Mouse Alexa Fluor 568 (IF, 1:500)	Thermo Fisher Scientific	AB_144696
Goat anti-Rabbit Alexa Fluor 488 (IF, 1:500)	Thermo Fisher Scientific	AB_2633280
Goat anti-Rabbit Alexa Fluor 568 (IF, 1:500)	Thermo Fisher Scientific	AB_143157
Goat anti-Rat Alexa Fluor 488 (IF, 1:500)	Thermo Fisher Scientific	AB_2534074
Goat anti-Mouse, VRDye 680 (WB, 1:10,000)	Li-COR Biosciences	AB_2651128
Goat anti-Rabbit, VRDye 800 (WB, 1:10,000)	Li-COR Biosciences	AB_2651127
Anti-Lrp2 polyclonal antibody (FC, 0.01mg/ml)	Thermo Fisher Scientific	AB_10884959
Moust anti-CD11c (FC, 0.01mg/ml)	BioLegend	RRID: AB_313776
Mouse anti-F4/80 (FC, 0.01mg/ml)	BioLegend	AB_893489
Mouse anti-CD45 (FC, 0.01mg/ml)	BioLegend	AB_312978
Mouse anti-CD3 (FC, 0.01mg/ml)	BioLegend	AB_10898314
Mouse anti-NK1.1 (FC, 0.01mg/ml)	BioLegend	AB_2562216
Rabbit anti-YAP (IF, 1:100)	Cell Signaling Technology	AB_2650491
Rabbit anti-TAZ (IF, 1:200)	Cell Signaling Technology	AB_10950494
Rabbit anti-pTAZ (phospho S311) (IF, 1:100)	Abcam	AB_3752596
Rabbit anti-pYAP (phospho S127) (IF, 1:250)	Abcam	AB_1524578
Rabbit anti-Cleaved Caspase 3 (IF, 1:400)	Cell Signaling Technology	AB_2341188
Rabbit anti-phospho Histone H3 (IF, 1:200)	Sigma-Aldrich	AB_310177
Bacterial and virus strains		
DH5a	NEB	C2987H
Chemicals, peptides, and recombinant proteins		
Trizol RNA extraction reagent	Invitrogen	15596026
Bullseye Real Time qPCR master mix EvaGreen	MidSci	BEQPCR-S
Carbenicillin disodium salt	Thermo Fisher Scientific	J61949.08
Kanamycin monosulfate	Alfa Aesar	J60668

Collagenase IV	Gibco	17104-019
Fetal bovine serum (FBS)	Gibco	A52567-01
Penicillin/streptomycin	Gibco	15140-122
L-Glutamine	Gibco	25030-081
Recombinant Human Insulin	MP Biomedicals	193900
Human transferrin	Sigma-Aldrich	T8158
Sodium selenite	Sigma-Aldrich	S9133
3,3,5'-Triiodo-Thyronine	Sigma-Aldrich	T6397
RIPA lysis buffer	Thermo Fisher Scientific	89901
Lipofectamine 3000 reagent	Invitrogen	L3000-015
Immobilon-FL transfer membranes	EMD Millipore	IPFL00010
ACK lysis buffer	Thermo Fisher Scientific	SCR_015963
Fc Block	BD Biosciences	Cat #553142
Tamoxifen	Sigma-Aldrich	T5648
10% SDS-polyacrylamide gels containing 1% gelatin	Novex	ZY00102BOX
EDTA-free protease inhibitor	Roche	11836170001
GelCode Blue	Thermo Fisher Scientific	24590
DQ Collagen type I From Bovine Skin, Fluorescein Conjugate	Invitrogen	D12060
Critical commercial assays		
Q5 Site-Directed Mutagenesis Kit	NEB	E0554S
ZymoPURE II plasmid midiprep kit	Zymo Research	D4200
High Capacity cDNA Reverse Transcription Kit	Thermo Fisher Scientific	4368814
Experimental models: Cell lines		
hTERT-RPE1	ATCC	CVCL_4388
ADAMTS9 KO RPE-1	Nandadasa et al., Nat. Comm (2019)	N/A
HEK293T	ATCC	CRL-3216
Experimental models: Organisms/strains		
Mouse: *Six2*$^{tm2(cre/ERT2)Amc}$/J (*Six2-Cre*)	UTSW O'Brien Kidney Research Core Center	JAX:032488

Mouse: *Adamts9*$^{tm1.1Apte}$/J (*Adamts9*$^{+/Fl}$)	Apte Laboratory	JAX:026103
Mouse: *Adamts9*$^{tm1.2Apte}$/Mmjax (*Adamts9*$^{+/Del}$)	Apte Laboratory	JAX:069571
Mouse: *Ift88*^{tm1Bky}/J *(Ift88*$^{+/Fl}$)	Jackson Laboratory	JAX:0220409
Mouse: *Tmem67em1*$^{(IMPC)J}$/Mmjax (*Tmem67 KO)*	Jackson Laboratory	MMRRC_051248-JAX
Mouse: *Tmem67*$^{\Delta CLE/+}$	Ahmed et al., Nat. Comm (2025)	N/A
Mouse: *Cdh16-Cre*^{91Igr}/J (*Ksp-Cre*)	Jackson Laboratory	JAX:012237
Mouse: *Vcan*$^{AA/+}$	Apte Laboratory	N/A
Mouse: *Vcan*$^{tm1.1Cwf}$ (*Vcan*$^{Fl/+}$)	Chuck Frevert Laboratory	MMRRC_068231-UCD
Mouse: *Pkd1*^{tm2Ggg}/J (*Pkd1*$^{Fl/+}$)	Jackson Laboratory	IMSR_JAX:010671
Mouse: *Pkd2*$^{tm1.1Tjwt}$/J (*Pkd2*$^{Fl/+}$)	Jackson Laboratory	IMSR_JAX:017292
Mouse: Tg(Hoxb7-Cre)13Amc/J	Jackson Laboratory	IMSR_JAX:004692
Mouse: *Gt(ROSA)26Sor*$^{tm1(Cre/ERT)Nat}$/J	Jackson Laboratory	IMSR_JAX:004847
Recombinant DNA		
ADAMTS9 Full-length pCDNA3.1 Myc/His	Apte Lab, Somerville et al., JBC (2003)	N/A
ADAMTS9 T65R C-Myc pENTER	Choi et al., AJHG (2019)	N/A
ADAMTS9 Q1525H N-Myc pENTER	Choi et al., AJHG (2019)	N/A
ADAMTS9 S636F pCDNA3.1 Myc/His	This paper	N/A
ADAMTS9 R647Q pCDNA3.1 Myc/His	This paper	N/A
ADAMTS9 C1024 pCDNA3.1 Myc/His	This paper	N/A
ADAMTS9 R1203W pCDNA3.1 Myc/His	This paper	N/A
ADAMTS9 P1655S pCDNA3.1 Myc/His	This paper	N/A
ADAMTS9 S1826N pCDNA3.1 Myc/His	This paper	N/A
Software and algorithms		
Image J FIJI	NIH	SCR_003070
LI-COR Acquisition (Ver 1.0)	Li-COR Biosciences	N/A
Leica Application Suite X (LAS-X)	Leica Microsystems	SCR_013673

GraphPad Prism (Ver 10.6.1)	GraphPad	SCR_002798
Bio-Rad CFX Maestro (Ver 2.3)	Bio-Rad	N/A
TissueFAX SL Viewer (Ver 7.1)	TissueGnostics	N/A

SUPPLEMENTAL MOVIE LEGENDS

Supplemental Movie 1 caption: Movie of 4-week-old male mice showing the distinctly small and hunched posture and abnormal gating of an *Adamts9* cKO mouse and two heterozygous littermates who are phenotypically and behaviorally normal.

Supplemental Movie 2 caption: Movie of female littermates of the male mice shown in supplemental movie-1, showing two *Adamts9* cKO and a heterozygous female at 4-weeks of age, who are visually and behaviorally normal and are indistinguishable from one another.

SUPPLEMENTARY FILE REFERENCES

1. Ahmed M, Fischer S, Robert KL, Lange KI, Stuck MW, Best S, et al. Cleavage of the Meckel-Gruber syndrome protein TMEM67 by ADAMTS9 uncouples Wnt signaling and ciliogenesis. *Nat Commun.* 2025;16(1):4946.
2. Dubail J, Aramaki-Hattori N, Bader HL, Nelson CM, Katebi N, Matuska B, et al. A new Adamts9 conditional mouse allele identifies its non-redundant role in interdigital web regression. *Genesis.* 2014;52(7):702-12.
3. Benz BA, Nandadasa S, Takeuchi M, Grady RC, Takeuchi H, LoPilato RK, et al. Genetic and biochemical evidence that gastrulation defects in Pofut2 mutants result from defects in ADAMTS9 secretion. *Dev Biol.* 2016;416(1):111-22.
4. Kobayashi A, Valerius MT, Mugford JW, Carroll TJ, Self M, Oliver G, et al. Six2 defines and regulates a multipotent self-renewing nephron progenitor population throughout mammalian kidney development. *Cell Stem Cell.* 2008;3(2):169-81.
5. Kang I, Harten IA, Chang MY, Braun KR, Sheih A, Nivison MP, et al. Versican Deficiency Significantly Reduces Lung Inflammatory Response Induced by Polyinosine-Polycytidylic Acid Stimulation. *J Biol Chem.* 2017;292(1):51-63.
6. Nandadasa S, Burin des Roziers C, Koch C, Tran-Lundmark K, Dours-Zimmermann MT, Zimmermann DR, et al. A new mouse mutant with cleavage-resistant versican and isoform-specific versican mutants demonstrate that proteolysis at the Glu(441)-Ala(442) peptide bond in the V1 isoform is essential for interdigital web regression. *Matrix Biol Plus.* 2021;10:100064.
7. Nandadasa S, O'Donnell A, Murao A, Yamaguchi Y, Midura RJ, Olson L, et al. The versican-hyaluronan complex provides an essential extracellular matrix niche for Flk1(+) hematoendothelial progenitors. *Matrix Biol.* 2021;97:40-57.
8. Bens M, Vallet V, Cluzeaud F, Pascual-Letallec L, Kahn A, Rafestin-Oblin ME, et al. Corticosteroid-dependent sodium transport in a novel immortalized mouse collecting duct principal cell line. *J Am Soc Nephrol.* 1999;10(5):923-34.
9. Nandadasa S, Kraft CM, Wang LW, O'Donnell A, Patel R, Gee HY, et al. Secreted metalloproteases ADAMTS9 and ADAMTS20 have a non-canonical role in ciliary vesicle growth during ciliogenesis. *Nat Commun.* 2019;10(1):953.
10. Choi YJ, Halbritter J, Braun DA, Schueler M, Schapiro D, Rim JH, et al. Mutations of ADAMTS9 Cause Nephronophthisis-Related Ciliopathy. *Am J Hum Genet.* 2019;104(1):45-54.
11. Peterson SM, Wang X, Johnson AC, Coate ID, Garrett MR, and Didion SP. Estimation of Nephron Number in Whole Kidney using the Acid Maceration Method. *J Vis Exp.* 2019(147).
12. Cebrian C, Asai N, D'Agati V, and Costantini F. The number of fetal nephron progenitor cells limits ureteric branching and adult nephron endowment. *Cell Rep.* 2014;7(1):127-37.
13. MacKay K, Striker LJ, Pinkert CA, Brinster RL, and Striker GE. Glomerulosclerosis and renal cysts in mice transgenic for the early region of SV40. *Kidney Int.* 1987;32(6):827-37.
14. Nandadasa S, Martin D, Deshpande G, Robert KL, Stack MS, Itoh Y, et al. Degradomic Identification of Membrane Type 1-Matrix Metalloproteinase as an ADAMTS9 and ADAMTS20 Substrate. *Mol Cell Proteomics.* 2023;22(6):100566.